Minerals Engineering 170 (2021) 107037

Contents lists available at ScienceDirect

Minerals Engineering

journal homepage: www.elsevier.com/locate/mineng

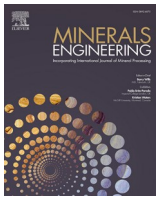

The effects of water recycling on flotation at a North American concentrator

A. Di Feo [a,*], C.M. Hill-Svehla [b], B.R. Hart [b], K. Volchek [a], L. Morin [a], A. Demers [a]

[a] CanmetMINING, Natural Resources Canada, 555 Booth Street, Ottawa, Ontario K1A 0G1, Canada
[b] Surface Science Western, University of Western Ontario, London, Ontario N6G 0J3, Canada

ARTICLE INFO

Keywords:
Multivariate analysis of variance
Flotation
Process water
Thickener tank overflow water
Recycling
Nickel
Copper
Recovery
Grade
ToF-SIMS
XPS
SEM/EDX

ABSTRACT

Due to environmental reasons and water shortage, concentrators have to increase water recirculation in the plant. The water originates from different sources, and depending on their origins, the water chemistry varies from stream to stream. Water chemistry has many significant impacts on flotation, beneficial or non-beneficial. Flotation tests have been conducted using process water (originates from tailings treatment facilities and is clean water that can be released to the environment) and thickener tank overflow water obtained from a North American concentrator. The concentrator would like to increase the recirculation of the thickener tank overflow water and reduce process water consumption. In this work, the flotation results between process water (PW) and thickener tank overflow water recirculated at various degrees were compared. Reverse osmosis (RO) at different degrees of recirculation (0%, 20%, 40%, 60% and 80% RO) was used to simulate water thickener tank overflow water recirculation. The results showed that higher pyrrhotite recoveries were obtained when thickener tank overflow water recirculated (0%, 20%, 40%, 60%, and 80% RO) was used compared to that obtained with process water. However, the pyrrhotite recovery did not increase between 0% and 20%, 40%, 60% and 80% RO. Relative to the process water, the higher pyrrhotite recovery using thickener tank overflow water at various degrees of recirculation did not appear to have been caused by a higher relative proportion of activating species on grain surfaces. Most likely, the higher pyrrhotite recovery in the thickener tank overflow water (0%, 20%, 40%, 60%, and 80% RO) relative to that of process water was due to higher bubble surface area flux (smaller air bubbles) caused by the higher total dissolved solids (TDS) relative to that of process water. Non-sulphide gangue (Ga) recovery was similar for all tests and was mainly due to water entrainment. The nickel and copper recoveries increased at 60% and 80% RO relative to that of process water, probably due to the higher bubble surface area flux generated by the higher total dissolved solids (TDS) in the recycled thickener tank overflow water. Pentlandite (nickel-bearing mineral) grains from the 80% RO and process water samples showed similar proportions of gangue species (e.g. calcium and magnesium) on their surfaces. However, nickel and iron oxide species were slightly higher on pentlandite from the 80% RO sample relative to the process water. The marginally higher amount of hydrophilic oxidative species on pentlandite from the 80% RO could perhaps account in part for the difference in flotation kinetics observed between the samples.

1. Introduction

Water is an essential component in mineral processing. Water is used as a method of transporting the mineral solids in grinding, flotation, and thickening. Managing water resources is essential because it affects the environment. In some countries, water is recycled due to water scarcity (Liu et al., 2013), and in other countries to prevent environmental pollution (Carlson et al., 2002).

Before water at a mine site is recycled, a strategy should be put in place. To establish this strategy, a study that includes samples taken over a long period has to be conducted to understand the chemistry of the streams (pH, ORP, ions in solution, etc.) (Di Feo et al., 2020). Equally, flotation testing to understand the impact of recycled water on metallurgy must be undertaken and replicated flotation tests for a rigorous statistical analysis (Di Feo et al., 2020; Le et al., 2020; Levay et al., 2001; Levay and Schumann, 2006). Surface analysis, for example ToF-SIMS and/or XPS, should explain the causes of paymetal recovery loss and accidental activation, if any, of gangue minerals. All this test work is to be compared to flotation tests done with clean water (Levay et al., 2001). If there is an improvement using clean water, then using water

* Corresponding author.
E-mail address: tony.difeo@canada.ca (A. Di Feo).

https://doi.org/10.1016/j.mineng.2021.107037
Received 25 February 2021; Received in revised form 2 June 2021; Accepted 15 June 2021
Available online 15 July 2021

treatment technologies should be considered. In this case, an economic study has to be performed to determine if it is economically feasible to implement water treatment technology. One of the advantages of water treatment technology is that it will provide consistent water chemistry to avoid complicating operating conditions and compromise flotation performance (Rao and Finch, 1989).

Ionic species in solution have an impact on flotation performance. The effect of recycled water will be different for every concentrator. The reason is that not all recycled water is the same, and concentrators treat different ore types. Depending on the ions in solution, these will have different impacts on flotation (Biçak et al., 2012; Muzenda, 2010; Liu et al., 2013). Therefore, the effect of recycled water has to be investigated on a case-by-case basis. When a copper/zinc ore from Kidd Creek was floated in recycled water, tap and distilled water, recycling water was not detrimental and pyrite depression was enhanced in copper flotation due to the presence of thiosalts and calcium ions (Liu et al., 1993). Researchers have shown that the recovery of galena was marginally lower in the presence of calcium and sulphate ions using potassium amyl xanthate as a collector (Ikumapayi et al., 2012). These researchers also stated that calcium carbonate and calcium sulphate in the process water were adsorbed on the galena surfaces, which affected xanthate adsorption (Ikumapayi et al., 2012).

The thickener tank overflow water stream of the concentrator is currently recycled to the grinding circuit. The remainder of the water balance is made up of process water; this stream comes from the tailings treatment process and is clean enough to be discharged to the environment. For the concentrator in question, it is desirable that the quantity of process water is minimized and the thickener tank overflow water maximized has to be investigated. The thickener tank overflow water had a much higher total dissolved solids (TDS). It has been shown in laboratory tests that the nickel + copper grade versus nickel recovery curve decreased when this water was used. More precisely, the nickel + copper grade of the primary rougher concentrates (primary Cu/Ni rougher concentrates 1 and 2) decreased relative to that obtained with process water. The diluents consisted of pyrrhotite and gangue (non-sulphide gangue) minerals. Therefore, in this article, the results of ToF-SIMS, XPS, and SEM/EDX analyses on pyrrhotite, gangue (non-sulphide gangue-Ga) and pentlandite minerals from the primary rougher concentrates (combined concentrates 1 and 2) obtained from flotation tests with process water and recycled thickener tank overflow water (0%, 20%, 40%, 60% and 80% RO) will be presented. The objective was to determine the causes of increased pyrrhotite and gangue (non-sulphide gangue) recoveries when process water and thickener tank overflow water were used, in addition to investigating the link with pentlandite, pyrrhotite, and gangue flotation kinetics.

2. Experimental

A nickel-copper ore was obtained from a North American concentrator. This ore was crushed to minus 2 mm (10 mesh), blended, and split into 1 kg lots. Table 1 shows the external reference distribution for the ore. All the relative standard distributions (RSD) were less than 5%, which means that the sample was well blended. Nickel is in pentlandite ($(Fe,Ni)_9S_8$) and copper is in chalcopyrite ($CuFeS_2$). There is also 0.73% nickel in pyrrhotite (determined using the EPMA technique). In addition to pentlandite and chalcopyrite, this ore also contained pyrrhotite ($Fe_{(1-x)}S$ (x = 0 to 0.2)) and gangue minerals. The main gangue minerals (>2% by mass) determined by MLA consisted of anorthite, quartz, actinolite, albite, plagioclase, orthoclase, biotite, and ankerite + clay (Fe).

Table 1
External reference distribution.

	Ni (%)	Cu (%)	Fe (%)	Leco S (%)
Average	1.85	1.24	24.34	12.95
St. Dev.	0.05	0.02	0.45	0.25
RSD (%)	2.74	1.65	1.83	1.93

The 1 kg lots were ground to 56% passing 75 μm using a laboratory rod mill. The grinding media mass was 10.5 kg consisting of a mixture of mild steel and stainless-steel rods (30% 316 stainless steel and 70% mild steel). The percent solids used in grinding was 60% using the same water as that of flotation. 3.2 g of lime was added to the mill to keep the pH at ~9.2.

2.1. Reverse osmosis (RO)

The reverse osmosis apparatus by Seprotech was used to simulate thickener tank overflow water recirculation. Reverse osmosis is a process driven by the pressure that purifies water using a partially permeable membrane to separate ions in solution and larger suspended particles in water. Pressure is applied to the feed stream to overcome osmotic pressure, and the stream is passed through a membrane (Malaeb and Ayoub, 2011). There are two products obtained using reverse osmosis. These products are the permeate (clean water or lower quantity of ions in solution) and the concentrate (higher quantity of ions in solution relative to the feed). The various degrees of recirculation was the following: 0% RO or no recirculation, 20% RO (ions concentrated in 80% of the original volume of the tote), 40% RO (ions concentrated in 60% of the original volume of the tote), 60% RO (ions concentrated in 40% of the original volume of the tote), 80% RO (ions concentrated in 20% of the original volume of the tote). The flotation tests performed at 20%, 40%, 60%, and 80% RO were done using the concentrate product from reverse osmosis treatment. Fig. 1 illustrates the reverse osmosis flowsheet used to simulate water recycling.

Table 2 shows the chemistries, total dissolved solids (TDS), total inorganic carbon (TIC), total organic carbon (TOC), and total carbon (TC) for all the RO and process water types. The process water and RO concentrates (one of the reverse osmosis products with the concentrated ions) at 0%, 20%, 40%, 60%, and 80% RO were assayed. The total dissolved solids (TDS) increased as a function of reverse osmosis water recycling, and the highest TDS, sulphate, calcium, copper, potassium, sodium, sulphite, total organic carbon (TOC), and total carbon (TC) concentrations were obtained for 80% RO and the lowest concentrations of these species were obtained for process water. As the thickener tank overflow water was recirculated the ionic species increased due to the accumulation of ions in solution.

2.2. Flotation

The laboratory flotation tests were done at room temperature using process water and thickener tank overflow water obtained from a North American concentrator. Flotation tests were conducted at: (a) 100% process water, (b) thickener tank overflow water at 0% RO (no recirculation), and (c) thickener tank overflow water passed in reverse osmosis (RO) apparatus at various degrees (20%, 40%, 60% and 80% RO) of recirculation.

A Denver flotation machine and a 2-litre cell were used. Fig. 2 shows the laboratory flotation diagram (pyrrhotite roughers are considered to be scavengers). The products of the flotation tests were the following: primary copper (Cu)/nickel (Ni) rougher concentrates 1 and 2, secondary Cu/Ni rougher concentrates 3 and 4, pyrrhotite rougher concentrates 1 and 2, and tailings. The flotation times for the consecutive concentrates were 1, 1, 2, 2, 4, and 4 min, respectively, for a total of 14 min. In the primary and secondary Cu/Ni rougher concentrates, the objective was to float pentlandite ($(Fe,Ni)_9S_8$) and chalcopyrite ($CuFeS_2$), followed by pyrrhotite ($Fe_{(1-x)}S$ (x = 0 to 0.2)) flotation in the scavengers (pyrrhotite roughers 1 and 2).

The rpm and air flowrate (compressed air) used were 1100 and 5 L/min, respectively. The froth depth was kept at 1 to 1.5 in., and the froth removal rate was 1 stroke for every 5 s. The pH for Cu/Ni flotation circuit (primary and secondary roughers) was adjusted to 9.2 using lime. Pyrrhotite was floated at pH 8.0 (pH was adjusted using sulphuric acid

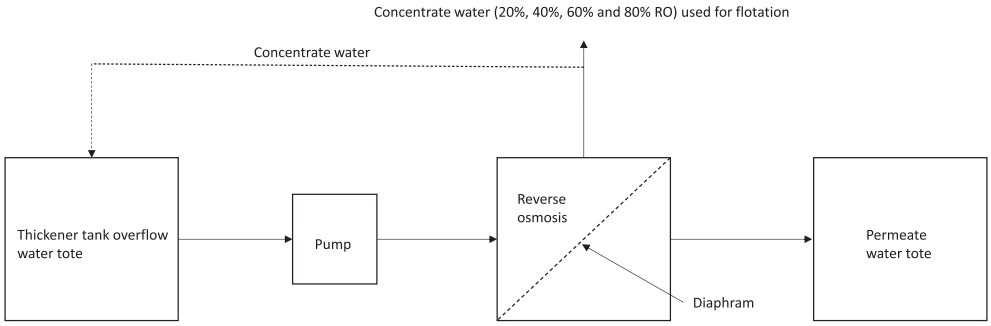

Fig. 1. Reverse osmosis (RO) setup.

Table 2
Water chemistry for process water and thickener tank overflow water (0% RO, 20% RO, 40% RO, 60% RO and 80% RO).

	TDS (mg/L)	SO_4^{2-} (mg/L)	Ca (mg/L)	Cu (mg/L)	K (mg/L)	Mg (mg/L)	Na (mg/L)	S (mg/L)	TIC (mg/L)	TOC (mg/L)	TC (mg/L)
Process Water	1138	627	263	0.019	22	16	80	210	9	3	12
0%RO	2268	6335	656	0.023	47	0.035	106	743	12	9	21
20%RO	2598	706	808	0.039	53	0.034	124	1011	14	14	28
40%RO	3388	945	979	0.056	60	0.031	147	1254	9	16	25
60%RO	4120	1153	1261	0.084	69	0.040	180	1568	9	24	33
80%RO	4760	1363	1754	0.092	91	0.037	252	2155	4	44	48

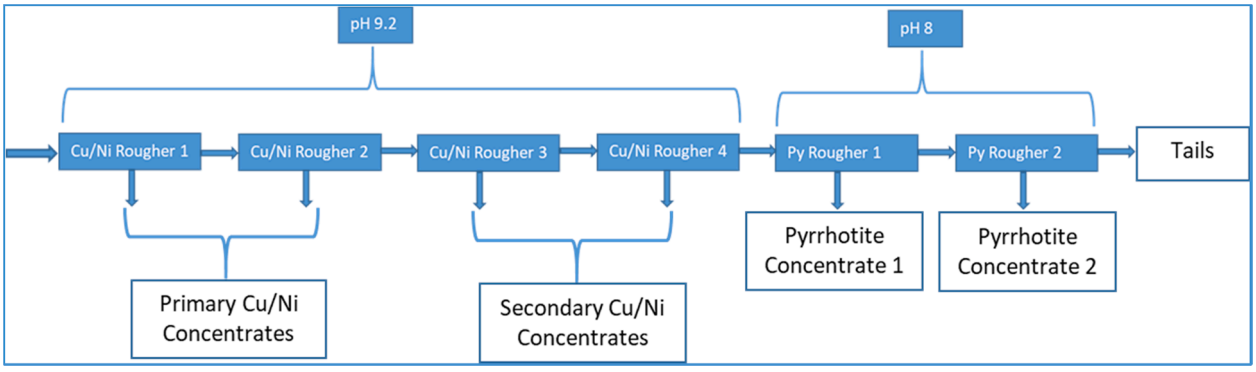

Fig. 2. Laboratory flotation diagram (rougher-scavenger flowsheet).

(10% dilution by mass with water)). The reagents used were potassium isobutyl xanthate as a collector (81.11% xanthate by weight) from Prospec chemicals and Polyfroth W31 as a frother (with a maximum of 0.5% water) from Quadra Chemicals. The dosage of potassium isobutyl xanthate and Polyfroth W31 were 86.5 g/t and 40 g/t, respectively. The concentrates and tails were assayed for nickel, copper, iron, and sulphur. Nickel, copper, and iron were assayed using the microwave digestion method followed by inductively coupled plasma-optical emission spectroscopy (Agilent Technologies, Model 5110 VDV), and sulphur was assayed using the Leco method. The flotation tests were done in triplicate.

2.3. ToF-SIMS

The Time-of-Flight Secondary Ion Mass Spectrometry (ToF-SIMS) technique is a comparative study that provides a comprehensive survey of surface species, including reagents, potential activators, and oxidative species, on the top monolayer of mineral grains of interest in the samples. For the ToF-SIMS analysis, samples of the flotation streams were collected in situ during testing and frozen immediately using dry ice, then shipped to Surface Science Western for analysis. A minimum of 25 grains of interest per sample was examined. The samples were prepared one at a time by rinsing a portion of the frozen sample into a clean glass vial. The collected material was rinsed repeatedly with deionized water, shaken, and decanted to remove fine-grained material that may interfere with the analysis. Grains were selected using an optical microscope and mounted on indium foil for analysis.

To identify potential surface chemical factors related to the flotation performance of the recirculated water samples, a ToF-SIMS surface analysis was undertaken on the combined primary Cu/Ni rougher concentrates 1 and 2. The IONTOF ToF-SIMS IV™ secondary ion mass spectrometer was used to analyze pyrrhotite, gangue (non-sulphide gangue), and pentlandite grains from primary Cu/Ni rougher concentrate samples (combined primary concentrates 1 and 2). For each sample, a minimum of 25 regions of interest (ROI) representing grains of each pyrrhotite, gangue (non-sulphide gangue), and pentlandite were examined. The data were collected using a 25 kV clustered Bi^{3+} primary ion beam over a raster area of approximately 300 × 300 μm. It should be noted that the corresponding tailings samples were not available for analysis. So the cause for the overall reduction in grade can only be inferred from the observed surface chemical factors identified from the primary rougher concentrate samples.

2.4. SEM/EDX analysis

The scanning electron microscopy coupled with energy-dispersive x-ray spectroscopy (SEM/EDX) analysis was carried out on pyrrhotite grains from the process water (PW), 0%, 40%, and 80% RO samples and

pentlandite from the process water, 40% RO and 80% RO samples to investigate the potential presence of physical precipitates on the surface of the grains. A minimum of 20 Fe-sulphide and pentlandite grains from each sample were mounted on carbon adhesive disks and preliminary analyses using EDX were completed to confirm their composition. Selected grains were further imaged using a Hitachi SU8230 Regulus field emission scanning electron microscope (FE-SEM) combined with a Bruker FlatQuad SDD Energy Dispersive X-ray (EDX). A 5 kV electron accelerating voltage was used for the analyses.

2.5. XPS analysis

The x-ray photoelectron spectroscopy (XPS) analyses were carried out on pyrrhotite from the process water (PW), 0%, 40%, and 80% RO samples, and on pentlandite from the PW, 40% RO, and 80% RO samples to identify surface oxidation species on the grains. A Kratos AXIS Supra X-ray photoelectron spectrometer was used to conduct the analyses. Survey spectra were obtained from approximately 300 × 700 μm area using a pass energy of 160 eV. XPS high-resolution spectra were obtained from approximately 300 × 700 μm area using a pass energy of 40 eV. Note that carbon and oxygen associated with the adhesive used to mount the grains for analysis were detected in the survey spectra. However, this should not pose a problem as we are concerned with iron, nickel, and sulphur oxidation.

3. Statistical analysis

A multivariate analysis of variance (MANOVA) using blocking was performed to establish which of the water types possibly affect the nickel, copper, pyrrhotite, and gangue recoveries in primary rougher concentrate 1 and cumulative nickel and copper recoveries for the rougher-scavenger test (Fig. 2). Multivariate analysis of variance (MANOVA) is an extension of the analysis of variance (ANOVA). MANOVA helps us evaluate whether multiple levels of independent variables affect the response variables on their own or in combination with one another. Whereas, in ANOVA, differences among various group means on a single-response variable are studied, in MANOVA, the number of response variables can be increased to two or more. For this study, the MANOVA analysis results were obtained using SAS software.

The family-wide error used was 5% (family confidence of 95%). The Bonferroni adjustment was used in testing the significance of the effects. The Bonferroni correction was required to adjust the probability (α) values because of the increased risk of a type 1 error when making multiple statistical tests, as we did in this case. In the Bonferroni adjustment, the intent is to reduce the likelihood of finding an erroneous statistically significant effect (purely by random chance); the family-wide confidence level can be represented as $1\text{-}\Sigma\alpha_i$ where α_i represents the confidence for every variable. Let us suppose that $\alpha = 0.05$ and two comparisons are considered in the statistical analysis. Hence, we test the significance at $0.05/2 = 0.025$ (α/m) where m is the number of comparisons because of the Bonferroni adjustment. The α/m (0.05/m) ratio was compared to the probability > F statistic (Pr > F, which is equivalent to p-value) in the SAS output. If Pr > F (SAS output) was less than 0.05/m, then the factor in question was statistically significant at the 95% level. The methodology is described in Johnson and Wichern (2019).

The requirements for MANOVA are the following: The data from the group has a common mean vector (no sub-populations), the observations have to be independent, the data distribution has to be normal, and the variance has to be constant. These conditions were verified before performing the MANOVA analysis and are not shown in this article. These conditions were met for all the tests (nickel, copper, pyrrhotite, and gangue recoveries in primary rougher concentrate 1 and cumulative recoveries of nickel and copper for a rougher-scavenger test). Unfortunately, the variance was not constant for the cumulative nickel, copper, pyrrhotite, and gangue recoveries in primary rougher concentrate 2, so the MANOVA could not be done for this concentrate. Thus, the Kruskal-Wallis test (non-parametric test) was used for the cumulative nickel, copper, pyrrhotite, and gangue recoveries in primary rougher concentrate 2. The SAS software was used for the Kruskal-Wallis testing (He, 2013). The null and alternate hypothesis tests used in the analysis of the test work results are shown in the Appendix A.

4. Flotation parameters

The method described by Napier-Munn (2012) was used to establish the maximum recovery (R_m (%)), the first-order rate constant (k (min^{-1})), and the significance of these parameters between process water and the percentage thickener tank overflow water recycled (simulated using reverse osmosis-0%, 20%, 40%, 60% and 80% RO for flotation tests).

$$R_t = R_m\left(1 - e^{-kt}\right) \quad (1)$$

where R_t is the recovery (%) at time t (minutes), R_m is the maximum recovery (%), and k is the first-order rate constant (min^{-1}). The significance of the maximum recovery (R_m) and flotation rate constant (k) between the process water and the percent thickener overflow tank water (%RO) recycled was done using the method proposed by Napier-Munn (2012), with the exception that 100 simulations were used in MCSimsolver.

5. Process description

Fig. 3 illustrates the block flow diagram of the process. The flowsheet consists of two grinding lines (lines A and B) in parallel and two rougher flotation lines in parallel (Side A and Side B). The concentrator would like to increase the recirculation of the thickener tank overflow water stream (the % solids are <0.5%) and decrease process water utilization. Thus, if the recirculation of the thickener tank overflow water is increased, the ionic species concentration will increase, which can affect flotation performance.

6. Results

6.1. Flotation

Fig. 4 shows the nickel + copper grade versus nickel recovery for the various types of water tested. The results are the average of three tests. The nickel + copper grade versus nickel recovery curve for process water was higher than those obtained with the thickener tank overflow water at various degrees of recirculation due to lower pyrrhotite recovery (Fig. 5). In addition, the nickel recoveries for the primary Cu/Ni rougher 1 at 0% RO, 20% RO, 40% RO, 60% RO and 80% RO were lower than those obtained with process water (statistical testing will be discussed shortly). The surface analyses showed that there were gangue surface species present on the pentlandite surfaces, which will be discussed later, in the combined primary Cu/Ni rougher concentrates 1 and 2 causing the lower nickel recoveries.

Fig. 5 illustrates the pyrrhotite recovery versus pentlandite recovery. The cause for the lower nickel + copper grade (Fig. 4) for the thickener tank overflow water at various degrees of recirculation was due to higher pyrrhotite recovery.

Fig. 6 shows the non-sulphide gangue (Ga) recovery versus pentlandite recovery. All the curves overlap; thus, there is no statistically significant difference for the non-sulphide gangue (Ga) versus pentlandite (Pn) recoveries. This was confirmed using a MANOVA analysis which is discussed later.

Table 3 illustrates the results of the maximum recoveries (R_m (%)) and the flotation rate constants (k (min^{-1})) for the flotation results using process water (PW), thickener tank overflow water (0%, 20%, 40%, 60% and 80% RO). For pentlandite, the flotation rate constant for process

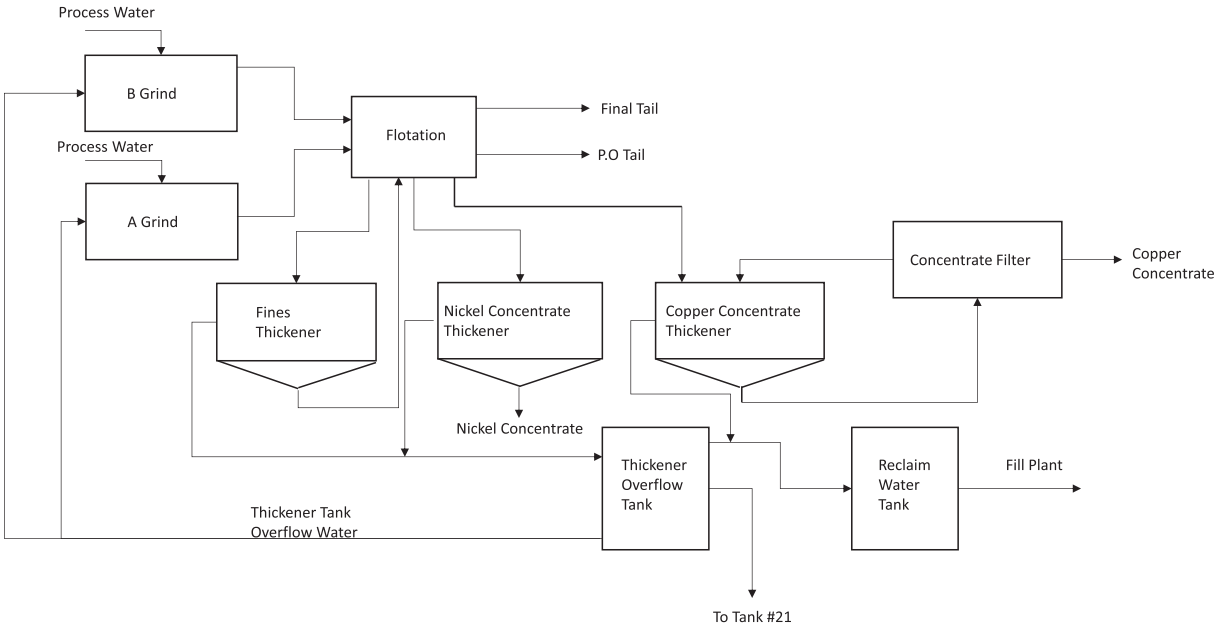

Fig. 3. Flowsheet of concentrator.

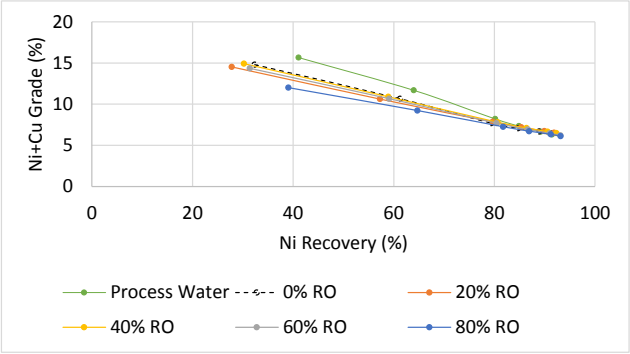

Fig. 4. Cumulative nickel + copper grade versus cumulative nickel recovery for process water and thickener tank overflow RO tests.

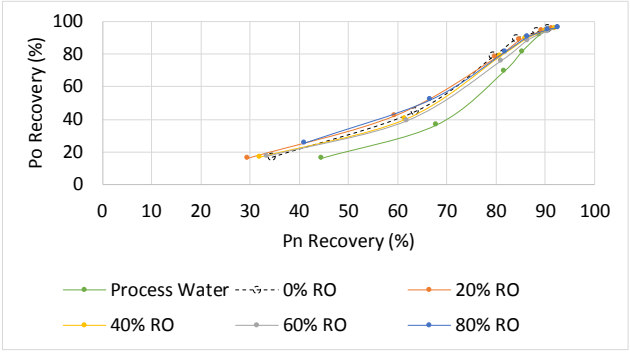

Fig. 5. Cumulative pyrrhotite recovery versus cumulative pentlandite recovery for process water and thickener tank overflow RO tests.

water (PW) was the highest. The recycled thickener overflow water (0%, 20%, 40%, 60%, and 80% RO) had a negative impact, lower flotation rate constant, on flotation kinetics. The flotation test conducted with 80% RO had the highest flotation rate constant relative to the other tests done with recycled thickener tank overflow water. For pyrrhotite, the opposite was observed. The flotation rate constants for the flotation tests

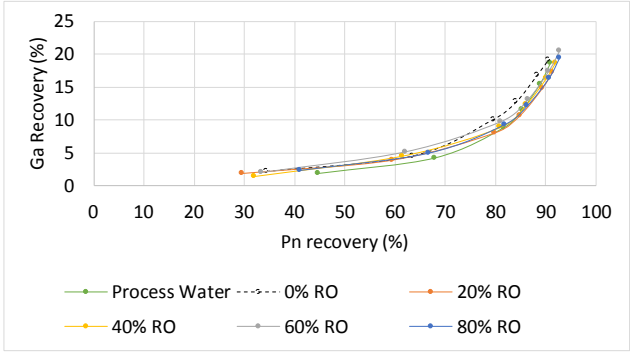

Fig. 6. Cumulative non-sulphide gangue recovery versus cumulative pentlandite recovery for process water and thickener tank overflow RO tests.

performed with thickener tank overflow water (0%, 20%, 40%, 60%, and 80% RO) were higher than that obtained with process water. For non-sulphide gangue (Ga) the flotation rate constants were similar for the tests done with process water and thickener tank overflow water (0%, 20%, 40%, 60%, and 80% RO). The significance of the differences of the maximum recovery and flotation rate constants obtained with process water and thickener tank overflow water (0%, 20%, 40%, 60%, and 80% RO) will be discussed shortly.

Table 4 shows the significance of the difference of maximum recoveries (R_m) and flotation rate constants (k) between process water (PW) and thickener tank overflow water (0%, 20%, 40%, 60%, and 80% RO). The symbol Δ means the difference. Since we are looking for an increase between the maximum recovery (Rm) and flotation rate constant (k), a 1-sided test was used. For pentlandite, the difference in maximum recoveries between PW and 40% RO and 60% RO were statistically significant ($P(z) < 0.05$). Thus, we can reject the null hypothesis (Eqs. (6) and (8) in the Appendix A). Since the differences were negative, the maximum recovery of pentlandite using PW was lower than those obtained with 40% RO and 60% RO. For pentlandite, the differences of the flotation rate constants between PW and those for the thickener tank overflow water (0%, 20%, 40%, 60%, and 80% RO) were positive and significant ($P(z) < 0.05$). Therefore, we can reject the null hypothesis (Eqs. (32), (34), (36), (38) and (40) in the Appendix A). This

Table 3
Maximum recovery and flotation rate constants for pentlandite, pyrrhotite and gangue.

Pentlandite (Pn)		
	R_m (%)	k (min^{-1})
PW	88.69	0.700
0% RO	89.19	0.555
20% RO	91.08	0.480
40% RO	91.48	0.509
60% RO	91.85	0.516
80% RO	90.66	0.621
Pyrrhotite (Po)		
	R_m (%)	k (min^{-1})
PW	99.56	0.260
0% RO	99.65	0.321
20% RO	100.00	0.310
40% RO	100.00	0.307
60% RO	100.00	0.295
80% RO	98.51	0.381
Non-sulphide gangue (Ga)		
	R_m (%)	k (min^{-1})
PW	23.76	0.109
0% RO	22.96	0.132
20% RO	22.25	0.108
40% RO	23.57	0.117
60% RO	25.58	0.116
80% RO	23.95	0.118

implied that recycling of the thickener tank overflow water reduced the flotation kinetics of pentlandite.

For pyrrhotite, the difference of the maximum recoveries between PW and thickener tank overflow water (0%, 20%, 40%, 60%, and 80% RO) was not statistically significant ($P(z) > 0.05$). Thus, we cannot reject the null hypothesis (Eqs. (12), (14), (16), (18) and (20) in the Appendix A). However, the difference of the flotation rate constants between PW and thickener tank overflow water (0%, 20%, 40%, and 80% RO) was negative and statistically significant ($P(z)<0.05$). Thus, we reject the null hypothesis (Eqs. (42), (44), (46), and (50) in the Appendix A). This implied that the flotation rate constants for pyrrhotite obtained with thickener tank overflow water (0%, 20%, 40%, and 80% RO) were statistically significant higher than that obtained with PW. For non-sulphide gangue (Ga), the differences of the maximum recoveries and flotation rate constants between PW and thickener tank overflow water (0%, 20%, 40%, 60%, and 80% RO) were not statistically significant ($P(z) > 0.05$), which implied that recycled water did not affect the flotation of non-sulphide gangue (Ga). So we cannot reject the null hypothesis (Eqs. (22), (24), (26), (28), (30), (52), (54), (56), (58) and (60) in the Appendix A).

Water chemistry can have a significant impact on paymetal recovery (Liu et al., 2013). Therefore, a detailed MANOVA analysis was performed on the testwork. The results of the MANOVA analysis are shown below.

6.2. MANOVA

Two MANOVA analyses were done. The first MANOVA was performed on the nickel, copper, pyrrhotite (Po), and non-sulphide gangue (Ga) recoveries for the primary rougher concentrate 1 (first point on the nickel + copper grade versus nickel recovery curves in Fig. 4). The second MANOVA was done on the cumulative nickel and copper recoveries for the rougher-scavenger test (last point on the nickel + copper grade versus nickel recovery curves in Fig. 4).

Table 5 shows the results of the MANOVA on the effect of water type on nickel, copper, pyrrhotite and non-sulphide gangue recoveries for primary rougher concentrate 1 (Eq. (62) and alternate hypothesis in the Appendix A). The p-values were less than 0.05; thus, the nickel, copper, pyrrhotite, and/or non-sulphide gangue recoveries in primary rougher concentrate 1 were significantly (statistical) different between one or more water types. Table 6 illustrates the results of the MANOVA (orthogonal contrasts) for the effects of process water (PW) versus thickener tank overflow (0%, 20%, 40%, 60%, and 80% RO) for primary concentrate 1 (Eqs. (63)–(72) in the Appendix A). There were a total of five comparisons (process water versus thickener tank overflow at 0%, 20%, 40%, 60%, and 80% RO), so the Bonferroni adjustment used was five. The p-values in these tables were compared to $\alpha = 0.05/5 = 0.01$. All of the p-values in Table 6 were <0.01, thus, the nickel, copper, pyrrhotite, and/or non-sulphide gangue recoveries were significantly (statistical) affected between process water and thickener tank overflow water (0%, 20%, 40%, 60% and 80% RO). The analysis of variance (ANOVA) was used to determine whether nickel, copper, pyrrhotite, and/or gangue recoveries were significantly affected (statistical). The results of the ANOVA are shown in Table 7.

6.3. ANOVA

Table 7 shows the results of the ANOVA analysis for nickel, copper, pyrrhotite, and gangue (non-sulphide) recoveries. There were five comparisons; therefore, the Bonferroni adjustment used was five. The p-values were compared to $\alpha = 0.05/5 = 0.01$. For nickel recovery, the conditions process water (PW) versus 0% RO, process water (PW) versus 60% RO and process water (PW) versus 80% RO were not statistically significant ($p > 0.01$), so the null hypothesis was not rejected or there was not enough evidence to reject the null hypothesis (Eqs. (73), (79) and (81) in the Appendix A). For copper recovery, all the p-values were higher than 0.01, thus, the null hypothesis (Eqs. (83), (85), (87), (89), and (91) in the Appendix A) were not rejected or there was not enough evidence to reject the null hypothesis. For pyrrhotite recovery, the only statistically significant comparison was process water (PW) versus 80% RO (p-value < 0.01). For the other comparisons, the null hypothesis was not rejected (Eqs. (93), (95), (97), and (99)) or there was not enough evidence to reject the null hypothesis. The gangue recoveries between process water and thickener tank overflow (0%, 20%, 40%, 60%, and 80% RO) were not statistically significant (p-value > 0.01). The null hypothesis (Eqs. (103), (105), (107), (109), and (111)) were not rejected or there was not enough evidence to reject the null hypothesis.

As mentioned in the statistical analysis section, the variance for the primary rougher concentrate 2 (second point on Ni + Cu grade versus Ni recovery in Fig. 4) cumulative nickel, copper, pyrrhotite, and non-sulphide gangue was not constant. Therefore, one of the requirements of the MANOVA was not met. In this case, the Kruskal-Wallis test (non-parametric test) can be used for multivariate analysis. Table 8 shows the results of the Kruskal-Wallis test for primary rougher concentrate 2 for cumulative recoveries of nickel, copper, pyrrhotite, and non-sulphide gangue. The p-values were <0.05 for all test statistics. Hence, we can reject the null hypothesis (Eq. (144) in the Appendix A). This implied that at least one recovery for a water type was significantly (statistically at 95%) different from another recovery for another water type.

The Kruskal-Wallis analysis also computes the results for the effect of water type on each of the recoveries (nickel, copper, pyrrhotite, and gangue); the results are shown in Table 9. The p-values for nickel and pyrrhotite were statistically significant (p-value < 0.05). This implied that for at least one water type, the nickel and pyrrhotite cumulative recoveries in primary rougher concentrate 2 were significantly different. Unfortunately, the Kruskal-Wallis test cannot determine which water types caused significant differences (statistical) in recoveries. However, referring to Fig. 4, the primary rougher concentrate 2 nickel recoveries for thickener tank overflow water (0%, 20%, 40%, and 60% RO) tended to be lower than that for process water. Thus, most likely, the nickel recovery obtained with process water was higher than those obtained with thickener tank overflow (0%, 20%, 40%, and 60% RO). The nickel recovery obtained with 80% RO was similar to that obtained with process water, so most likely, these were not statistically different. Similar

Table 4
Significance results of maximum recovery and flotation rate constants for pentlandite, pyrrhotite, and gangue.

Pentlandite (Pn)						
	Mean Δ in R_m (%) between PW and %RO	Mean Δ in k (min^{-1}) between PW and %RO	z-test for R_m between PW and %RO	z-test for k between PW and %RO	1-sided P(z) for R_m between PW and %RO	1-sided P(z) for k between PW and %RO
PW	–	–	–	–	–	–
0% RO	−0.69	0.15	0.56	4.18	0.288	0.000
20% RO	−2.20	0.22	1.32	5.60	0.094	0.000
40% RO	−2.69	0.19	1.98	5.06	0.024	0.000
60% RO	−3.28	0.19	2.64	5.07	0.004	0.000
80% RO	−1.39	0.08	1.52	1.98	0.065	0.024
Pyrrhotite (Po)						
	Mean Δ in R_m (%) between PW and %RO	Mean Δ in k (min^{-1}) between PW and %RO	z-test for R_m between PW and %RO	z-test for k between PW and %RO	1-sided P(z) for R_m between PW and %RO	1-sided P(z) for k between PW and %RO
PW	–	–	–	–	–	–
0% RO	0.04	−0.07	0.01	2.55	0.494	0.005
20% RO	0.02	−0.05	0.01	1.87	0.497	0.031
40% RO	−0.01	−0.05	0.00	1.86	0.499	0.031
60% RO	−0.35	−0.04	0.14	1.39	0.444	0.082
80% RO	0.12	−0.12	0.05	6.23	0.480	0.000
Gangue (Ga)						
	Mean Δ in R_m (%) between PW and %RO	Mean Δ in k (min^{-1}) between PW and %RO	z-test for R_m between PW and %RO	z-test for k between PW and %RO	1-sided P(z) for R_m between PW and %RO	1-sided P(z) for k between PW and %RO
PW	–	–	–	–	–	–
0% RO	0.84	−0.02	0.49	1.53	0.630	0.130
20% RO	0.83	0.00	0.27	0.19	0.394	0.426
40% RO	−0.15	−0.01	0.08	0.33	0.470	0.371
60% RO	−2.85	0.00	0.66	0.16	0.255	0.437
80% RO	−0.11	−0.01	0.06	0.66	0.476	0.256

Table 5
MANOVA output for the effect of water type on nickel, copper, pyrrhotite, and gangue recoveries for primary rougher concentrate 1.

Statistic	p-value (Pr > F)
Wilks' Lambda	0.0024
Pillai's Trace	0.0197
Hotelling-Lawley Trace	0.0030
Roy's Greatest Root	<0.0001

observations can be made with pyrrhotite (Fig. 5). The pyrrhotite recoveries in primary rougher concentrate 2 for thickener tank overflow water (0%, 20%, 40%, 60% and 80% RO) tended to be higher than that for process water; thus, it is most probable that the pyrrhotite recovery obtained with process water was lower (statistically significant) than those obtained with thickener tank overflow water (0%, 20%, 40%, 60% and 80% RO). For copper and gangue recoveries in primary rougher concentrate 2 were not statistically different between the water types.

Tables 10 and 11 illustrate the MANOVA for water type and contrast analysis, respectively, for the rougher-scavenger test (last points on the flotation curves in Fig. 4). In this MANOVA analysis, only the cumulative nickel and copper recoveries were considered because we wanted to determine whether there were paymetal losses in the rougher-scavenger tails. Table 10 illustrates the results of the MANOVA for water type. All

Table 6
MANOVA output (contrast) for the effect of process water versus 0%, 20%, 40%, 60%, and 80% RO on nickel, copper, pyrrhotite, and gangue recoveries for primary rougher concentrate 1.

Statistic	PW versus 0% RO p-value (Pr > F)	PW versus 20% RO p-value (Pr > F)	PW versus 40% RO p-value (Pr > F)	PW versus 60% RO p-value (Pr > F)	PW versus 80% RO p-value (Pr > F)
Wilks' Lambda	0.0031	0.0006	0.0043	0.0007	0.0006
Pillai's Trace	0.0031	0.0006	0.0043	0.0007	0.0006
Hotelling-Lawley Trace	0.0031	0.0006	0.0043	0.0007	0.0006
Roy's Greatest Root	0.0031	0.0006	0.0043	0.0007	0.0006

the p-values were < 0.05; thus, the nickel and/or copper recoveries in the rougher-scavenger test were statistically different between one or more water types. The null hypothesis (Eq. (113) in the Appendix A) was rejected. A contrast analysis in MANOVA (Table 11) was done to establish which water type had a statistically significant impact on nickel and/or copper recoveries.

Table 7
ANOVA analysis for nickel, copper, pyrrhotite, and gangue recoveries for primary rougher concentrate 1.

Contrast	Nickel recovery p-value (Pr > F)	Copper recovery p-value (Pr > F)	Pyrrhotite recovery p-value (Pr > F)	Gangue recovery p-value (Pr > F)
Process water versus 0%RO	0.0241	0.3010	0.7636	0.4905
Process water versus 20%RO	0.0020	0.4075	0.9615	0.9869
Process water versus 40%RO	0.0075	0.6770	0.7521	0.2980
Process water versus 60%RO	0.0140	0.0522	0.6764	0.8828
Process water versus 80%RO	0.5583	0.0238	0.0048	0.3199

Table 8
Kruskal-Wallis test for water type for primary rougher concentrate 2 for cumulative nickel, copper, pyrrhotite, and gangue recoveries.

Statistic	p-value (Pr > F)
Wilks' Lambda	0.0038
Pillai's Trace	0.0135
Hotelling-Lawley Trace	0.0104
Roy's Greatest Root	<0.0001

Table 9
Kruskal-Wallis test for primary rougher concentrate 2 for cumulative nickel, copper, pyrrhotite, and gangue recoveries.

Element/Mineral	p-value (Pr > F)
Nickel	0.0040
Copper	0.1324
Pyrrhotite	0.0131
Gangue	0.8077

Table 10
MANOVA output for the effect of water type on cumulative nickel and copper recoveries (rougher-scavenger test).

Statistic	p-value (Pr > F)
Wilks' Lambda	0.0002
Pillai's Trace	0.0049
Hotelling-Lawley Trace	<0.0001
Roy's Greatest Root	<0.0001

Table 11
MANOVA output (contrast) for the effect of process water versus 0%, 20%, 40%, 60% and 80% RO on cumulative nickel and copper recoveries for the rougher-scavenger test.

Statistic	PW versus 0% RO p-value (Pr > F)	PW versus 20% RO p-value (Pr > F)	PW versus 40% RO p-value (Pr > F	PW versus 60% RO p-value (Pr > F	PW versus 80% RO p-value (Pr > F
Wilks' Lambda	0.5519	0.2469	0.0129	0.0001	0.0002
Pillai's Trace	0.5519	0.2469	0.0129	0.0001	0.0002
Hotelling-Lawley Trace	0.5519	0.2469	0.0129	0.0001	0.0002
Roy's Greatest Root	0.5519	0.2469	0.0129	0.0001	0.0002

There were a total of five comparisons (process water versus thickener tank overflow water (0%, 20%, 40%, 60, and 80% RO)), so the Bonferroni adjustment used was five. The p-values in Table 11 were compared to $\alpha = 0.05/5 = 0.01$. The p-values for the comparisons process water versus 0% RO, process water versus 20% RO and process water versus 40% RO were >0.01. Therefore, the null hypothesis (Eqs. (114), (116) and (118)) cannot be rejected or we do not have enough evidence to reject it. So 0% and 20% and 40% RO did not significantly affect the nickel and copper recoveries compared to those of process water. The comparisons between process water and 60% and 80% RO were statistically significant. Thus, for the comparisons between process water and 60% and 80% RO the null hypothesis can be rejected (Eqs. (120), and (122) in the Appendix A), so 60%, and 80% RO had a significant impact on nickel and/or copper recoveries in comparison to those of process water. In order to determine whether nickel and/or copper recoveries were affected (60% and 80% RO), an ANOVA was done (the ANOVA is part of the SAS program output when conducting a MANOVA contrast analysis).

6.4. ANOVA

Table 12 shows the results of the ANOVA analysis for cumulative nickel and copper recoveries for the rougher-scavenger test. There were five comparisons; therefore, the Bonferroni adjustment used was five. The p-values were compared to $\alpha = 0.05/5 = 0.01$.Appendix A In the MANOVA analysis the process water versus 40% RO was not significant; thus, in the ANOVA it will not be considered significant even though the p-value is <0.01. The nickel and copper recoveries for 60% and 80% RO were significant.So we reject the null hypothesis (Eqs. (130), (132), (140) and (142) in the Appendix A) and conclude that there was a statistically significant difference in nickel and copper recoveries between these water types.

Fig. 7 shows the profile plot for the rougher-scavenger test conditions. For nickel recovery, the only statistically significant conditions were process water versus 60%, and 80% RO as discussed previously. There was about a 1.5% improvement in nickel recovery for 60% RO and 80% RO compared to that for process water.

For copper recovery, the conditions that resulted in statistically significant improvements in recovery were process water versus 60%, and 80% RO. The improvements in copper recovery were not as big as those obtained for nickel recovery. There was about a 1%, and 1.25% increase in copper recovery for 60% RO, and 80% RO, respectively, compared to that for process water.

To explain the higher pyrrhotite (Po) and possibly gangue (non-sulphide) recoveries in the concentrates, the recoveries of these minerals were plotted against water recovery.

Figs. 8 and 9 illustrate the pyrrhotite recovery versus water recovery and non-sulphide gangue (Ga) recovery versus water recovery, respectively, for the rougher-scavenger test. The pyrrhotite recovery versus water recovery did not follow a straight line; thus, the recovery of this

Table 12
ANOVA analysis for cumulative nickel and copper recoveries for rougher-scavenger test.

Contrast	Nickel recovery p-value (Pr > F)	Copper recovery p-value (Pr > F)
Process water versus 0% RO	0.2964	0.9479
Process water versus 20% RO	0.1517	0.1353
Process water versus 40% RO	0.0071	0.0083
Process water versus 60% RO	<0.0001	<0.0001
Process water versus 80% RO	<0.0001	0.0016

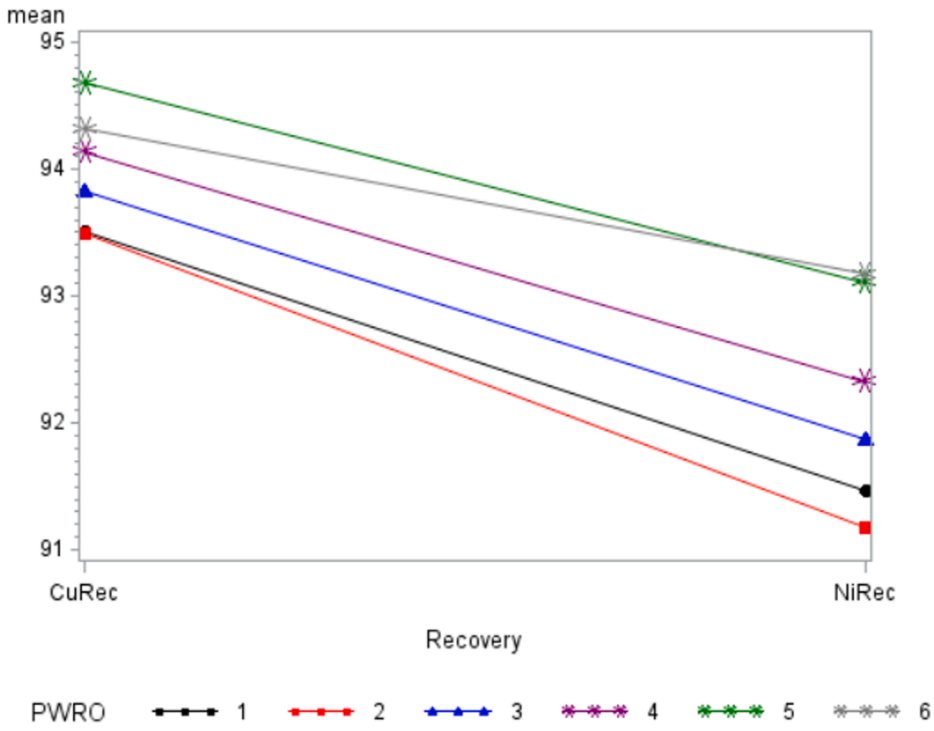

Fig. 7. Mean cumulative copper and nickel recoveries for rougher-scavenger test. 1 = process water, 2 = 0%RO, 3 = 20%RO, 4 = 40%RO, 5 = 60%RO and 6 = 80% RO (rougher-scavenger test).

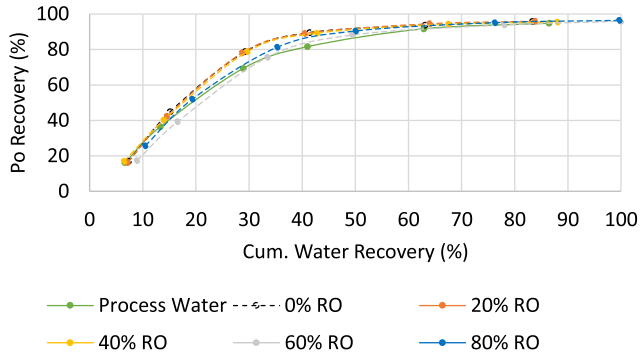

Fig. 8. Pyrrhotite recovery versus water recovery (rougher-scavenger test).

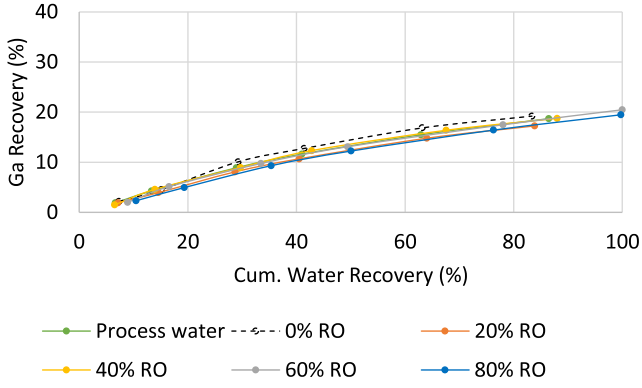

Fig. 9. Non-sulphide gangue recovery versus water recovery (rougher-scavenger test).

mineral was mainly due to true flotation. The pyrrhotite recovery versus water recovery was similar for all the water types. However, for the gangue (non-sulphide gangue-Ga) versus water recovery, the relationship between the two was reasonably linear for all water types. Therefore, the main recovery mechanism for gangue (non-sulphide gangue), for all water types, may be linked to an increase in water recovery; the mineral phases likely reporting to the concentrate as a result of entrainment.

7. Surface analysis

7.1. ToF-SIMS analysis

The ToF-SIMS analysis is non-quantitative because ion yields and the resultant intensities measured for the elements of interest are very different and dependent on the chemical environment in which the elements exist (matrix effect). The data is best used to demonstrate the presence or absence and relative proportion of species on a sample surface for comparative analysis. In regard to the data distribution, the discussion refers to a relative increase or decrease in measured species intensity between grains in the samples. Differences are subtle and typically fall over large ranges, commonly overlapping with comparison samples. Nonetheless, the differences are significant in that they illustrate potential factors linking the observed recoveries.

7.1.1. ToF-SIMS surface chemistry data presentation

The intensity of selected species, detected on the grain surfaces (also referred to as a region of interest ROI), as positive and negative ions are presented in vertical box plots (Figs. 10 and 11). All ToF-SIMS data presented (counts) are normalized by the total ion intensity (counts of the recorded total mass spectrum) for the region of interest. The normalization allows for comparison of different sized grain surface areas (ROIs).

As the data reflects the surface analysis from >25 grains, the data is typically highly variable. Therefore, for the comparative analysis between test samples, the normalized intensity data, plotted as vertical box

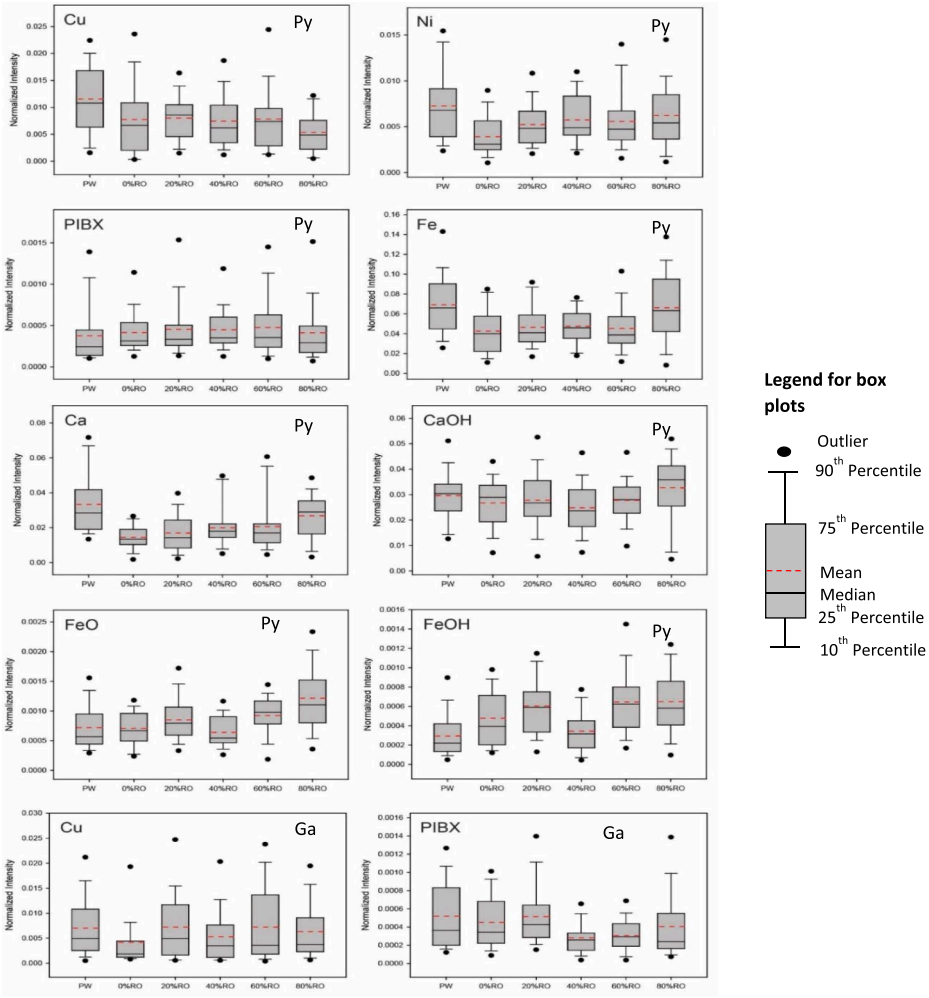

Fig. 10. Box plots showing normalized intensity of Cu, Ni, collector PIBX, Fe, Ca, CaOH, FeO and FeOH on pyrrhotite (Py) and gangue (Ga - non-sulphide gangue) surfaces from the process water and recycle water (thickener tank overflow water at 0%, 20%, 40%, 60% and 80% RO) samples.

plots, illustrates the relative changes in surface species abundance for the mineral grain examined in the sample. Relative differences in the discussion are based on the median values indicated in the figures we think better reflect the data. The mean tends to show significant influence by data set outliers. In the vertical box plots, the median is plotted as the solid line across the box whereas the mean is plotted as the dashed line.

7.1.2. Pyrrhotite and Non-sulphide gangue (Ga)

The data in Fig. 10 shows slightly higher relative intensities for Ni and Cu on the surface of pyrrhotite grains in the process water (PW) sample. But it shows higher relative intensity for Fe on the surface of pyrrhotite (Py) grains from the process water and 80% RO samples. The Fe distribution would suggest that the pyrrhotite grains from the process water and 80% RO samples have cleaner surfaces relative to the other samples. However, the process water and 80% RO samples show greater relative intensities for Ca and, in the 80% RO sample, CaOH (Fig. 10). Curiously, the intensity distribution of PIBX specie is slightly lower on grains from the process water and 80% RO samples relative to the others. However, variability between the test samples does not appear to be significant (Fig. 10).

Except for the 40% RO sample, the intensities of FeO and FeOH were higher on pyrrhotite in the recycled water samples relative to the process water sample (Fig. 10). Pyrrhotite oxidizes easily (Becker et al., 2010; Ekmekçi et al., 2010), and typically the presence of oxidative species on the surface of grains would promote depression. However, incomplete surface oxidation and development of hydrophobic species, such as metal deficient sulphides, polysulphides, and elemental S species, can potentially enhance pyrrhotite recovery (Kelebek et al., 2007; Multani and Waters, 2018).

The relevant species Cu and PIBX, which could promote non-sulphide gangue (Ga) flotation, are shown in Fig. 10. The data show no significant discriminating intensity for either species on the surface of the non-sulphide gangue (Ga) grains analysed between the various test samples.

It should be pointed out that the corresponding tailings samples were not available to compare the relative proportion of activator, collector, and oxidation species on the grains of interest; so we do not know whether the pyrrhotite or non-sulphide gangue grains reporting to the tailings have a greater or lesser proportion of these species on their surfaces. Overall, the data reveal that both sulphide and non-sulphide gangue grains reporting to the rougher concentrates had copper, nickel, and collector (PIBX) on their surfaces; suggesting that inadvertent flotation of both the pyrrhotite and non-sulphide gangue flotation is at least partly in response to activator and collector attachment.

7.1.3. Pentlandite

The surface analysis data from pentlandite grains (Pn) (Fig. 11) shows that the reported intensity of Ni and Fe are highest on grains from the 60% and 80% RO samples and lowest on grains from the 40% RO sample. The highest S surface intensity was seen on grains from the 80% RO sample. However, S intensity discrimination between samples does

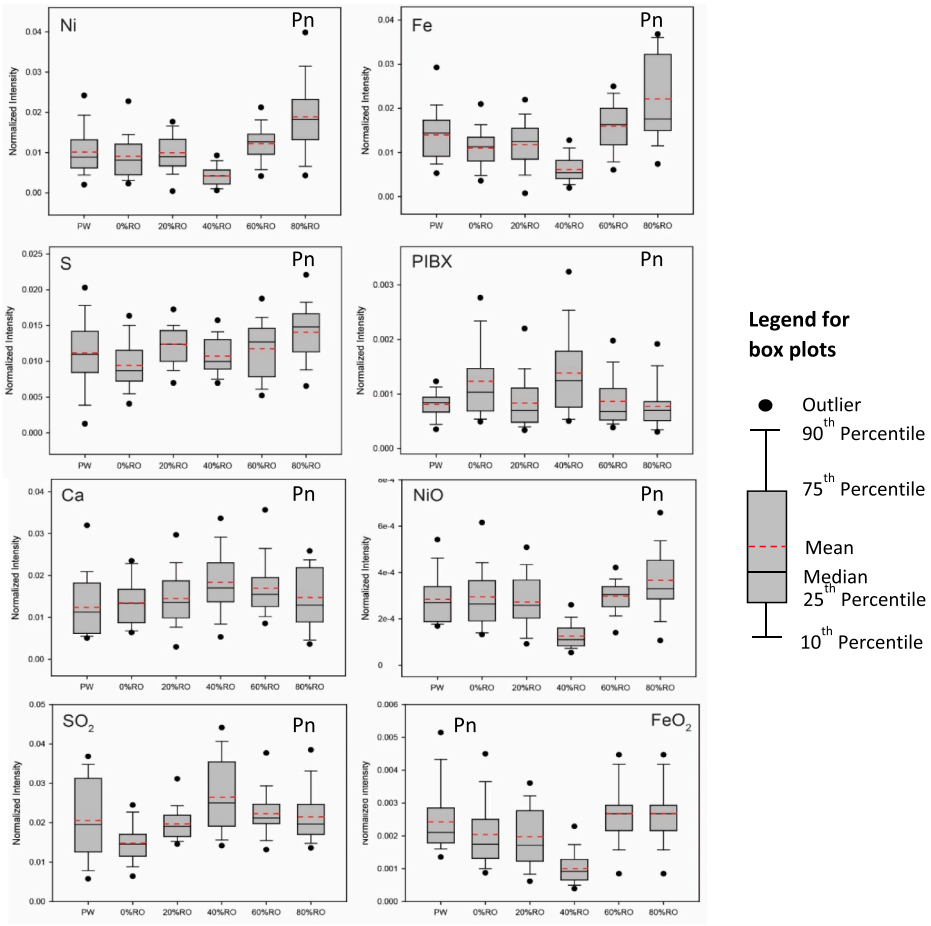

Fig. 11. Box plot showing the normalized intensity of Ni, Fe, S, collector PIBX, Ca, NiO, SO_2, and FeO_2 on pentlandite surfaces from the process water and recycle water (thickener tank overflow water at 0%, 20%, 40%, 60% and 80% RO) samples.

not appear to be significant overall. The highest reported surface intensities of the collector species were reported from the 0% and 40% RO samples, whereas the other samples showed similar levels of collector intensities. The hydrophilic species, Ca shown here but similar distributions were noted for Mg, Na, K, and Al, are slightly higher on pentlandite grains from all RO samples, but most notably from the 20%, 40%, and 60% RO samples. Nickel (Ni) and iron (Fe) oxide species are marginally higher on pentlandite grains from the 60% and 80% RO samples, whereas for the 40% RO sample, the intensity is significantly lower. The relative intensity of sulph-oxy species, represented here by SO_2, is highest on pentlandite grains from the 40% RO sample compared to the other samples.

Keeping in mind that tailings samples for pentlandite surface analysis comparison were not available, the current data suggest that the flotation of pentlandite is facilitated by collector adsorption. The high relative proportion of nickel (Ni), iron (Fe), and sulphur (S) on pentlandite, in addition to the higher relative proportion of both Ni and Fe oxide species from the 60% RO and 80% RO samples may suggest that recovery, as with pyrrhotite, is facilitated by partial oxidation and development of hydrophobic polysulphides and elemental S species on the surface of the grains. The overall increase in the relative proportion of inorganic species, such as Ca, Na, and K, likely reflects the increased proportion of these species in the concentrated recycled thickener overflow water (Table 2).

Additional analyses of selected samples by XPS and high-resolution SEM/EDX were performed to identify oxidation species and investigate the potential presence of physical precipitates on the surface of the grains, which may be linked to their flotation performance.

7.2. XPS analysis

For pyrrhotite, initial attempts to use XPS imaging to select grains for analysis were unsuccessful, so larger areas centered on specific grains were used. The survey spectra of grains from the 40% RO and process water samples showed a poor Fe resolution, which made discrimination between pyrrhotite and pyrite grains difficult in these samples. However, we believe that the surface processes affecting these mineral phases would be similar. For pentlandite, groupings of 10 to 12 pentlandite grains were analyzed from each of the selected samples.

7.2.1. Pyrrhotite

Survey spectra results for pyrrhotite in atomic percent are presented in Table 13. The lack of Ni and Cu identified in the XPS analysis of pyrrhotite reflects the relatively low proportion of these surface adsorbed components and the significantly higher surface sensitivity and lower detection limits of the ToF-SIMS technique. Pyrrhotite grains from the 40% RO sample had a more significant proportion of Ca, Cl, K, Na, O, and Si on their surfaces relative to grains from the process water, 0% RO, and 80% RO samples.

Grains from the process water and 40% RO samples had a greater proportion of S present as sulphate and sulphite species relative to the 80% RO sample (Fig. 12). Pyrrhotite from the 0% RO and 80% RO samples had 38% and 67% of S present as sulphide, respectively, and show significantly fewer secondary S (SO_X) species on their surfaces relative to grains from the other three analyzed samples. All three RO samples had similar Fe 2p results, with between 52 and 54% of the Fe present as pyrrhotite and 46–49% present as Fe-oxide, Fe-sulphite, or Fe-sulphate species (Fig. 12). This trend is reversed for the process water

Table 13
Results of XPS analyses of the surface elemental composition of pyrrhotite in atomic percent (combined primary rougher concentrates 1 and 2).

Sample	C	Ca	Cl	Fe	K	N	Na	O	S	Si
PW – Grain 1	76.7	1	–	0.1	–	2.3	0.2	17.8	1.2	0.8
PW – Grain 2	80.5	0.4	–	0.1	–	2.4	0.3	14.5	0.7	1
0% RO – Grain 1	80.2	0.5	–	0.3	–	2.8	0.2	14.5	1.3	0.3
0% RO – Grain 2	81.8	0.6	–	0.4	–	2.5	0.4	12.5	1.1	0.6
40% RO – Grain 1	65.3	1.5	0.8	0.1	1.6	2.7	1.7	22.8	2.2	1.3
40% RO – Grain 2	68.1	1.5	0.8	0.2	1.3	3.1	1.7	20.4	1.9	1
80% RO – Grain 1	79.1	0.5	–	0.8	–	2.9	0.1	15.1	1.1	0.4
80% RO – Grain 2	81.9	0.3	–	0.7	–	3.2	0.4	12.2	0.9	0.4

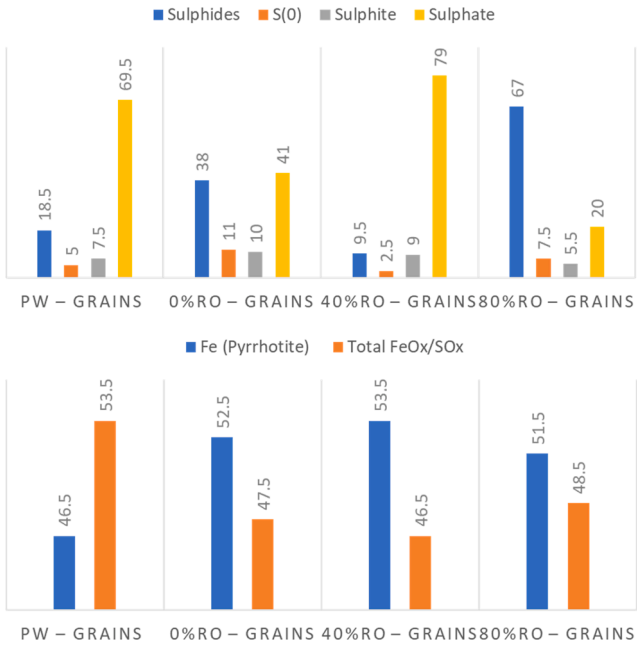

Fig. 12. Results of high-resolution S 2p (upper) and Fe 2p (lower) XPS analyses of pyrrhotite as a percentage of total sulphur and iron. Note the data shows the average of 2 pyrrhotite grains (combined primary rougher concentrates 1 and 2).

samples where the proportion of Fe as pyrrhotite is only 46% and the proportion of Fe as oxides or sulph-oxy species is around 53%.

7.2.2. Pentlandite

Survey spectra results for pentlandite in atomic percent are presented in Table 14. Except for Na, which shows twice the surface proportion on grains from the 40% RO sample, overall pentlandite grains from the process water, 40% RO, and 80% RO samples analysed have similar relative proportions of hydrophilic species on their surfaces.

High-resolution S 2p analysis (Fig. 13) indicates that the proportion of elemental sulphur, S(0), on the process water and 80% RO samples is approximately double that on the 40% RO sample. Furthermore, the relative proportion of sulphates is higher on the grains from the 40% RO samples. Pentlandite grains from the 40% RO and 80% RO samples show similar percentages of Fe present as pentlandite (12%) and secondary Fe

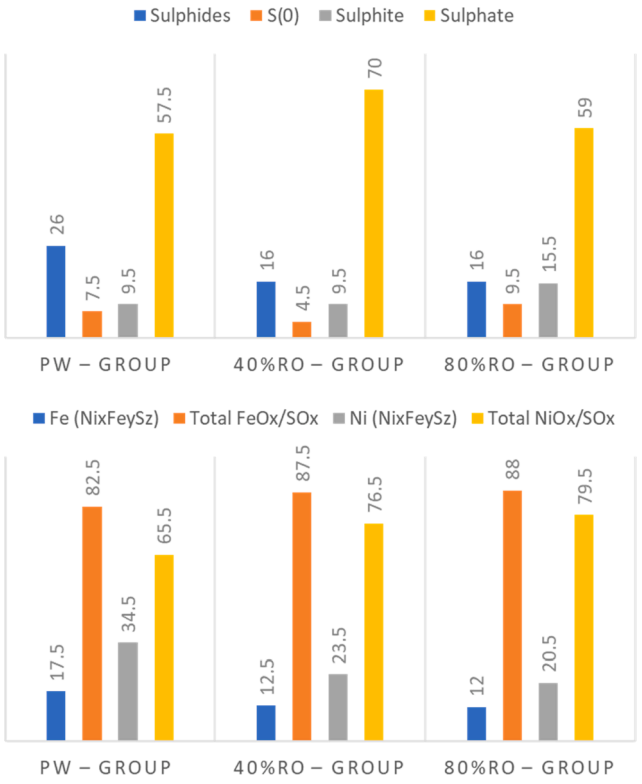

Fig. 13. Results of high-resolution S 2p, Fe 2p, and Ni 2p XPS analyses of pentlandite as a percentage of total sulphur, iron, and nickel, respectively. Note the data shows the average of groups of pentlandite grains (combined primary rougher concentrates 1 and 2).

species (87%); the process water (PW) sample has slightly higher Fe proportions at 18%. Grains from the 40% RO and 80% RO samples show similar percentages of Ni present as pentlandite (23% and 20%, respectively), with Ni on the grains from the PW sample at 17%. Both the total Fe and Ni oxide/sulphite/sulphate species are higher on the surface of pentlandite grains from the 40% and 80% RO samples.

The high-resolution S 2p, Fe 2p, and Ni 2p results support the contention that the formation of hydrophobic metal deficient sulphides, polysulphides, and elemental S, through the partial oxidation of pyrrhotite and pentlandite surfaces may have facilitated flotation.

Table 14
Results of XPS analyses of the surface elemental composition of pentlandite in atomic percent (combined primary rougher concentrates 1 and 2).

Sample	B	C	Ca	Cu	Fe	K	Mg	N	Na	Ni	O	S	Si
PW – Group 1	0.8	67.1	1	0.1	0.4	–	0.4	2.6	1	0.5	22.9	2.3	0.9
PW – Group 2	0.8	70.1	1	0.1	0.7	0.3	0.4	1.9	1	0.4	20.4	2	0.9
40%RO – Group 1	0.9	66.1	1.1	–	0.3	0.5	0.3	2	2.4	0.2	23.5	1.8	0.9
40%RO – Group 2	0.7	69.4	0.6	–	0.3	0.2	0.3	2.3	2.1	0.1	21.7	1.1	1.2
80%RO – Group 1	0.4	70.1	1.4	–	0.1	–	0.3	2.4	0.8	0.1	21.7	1.3	1.3
80%RO – Group 2	0.4	68.6	1.4	–	0.4	–	0.4	2.2	1.2	0.3	22.3	2	0.8

SEM/EDX analysis

7.2.3. Pyrrhotite

High-resolution SEM images, EDX elemental X-ray intensity maps, and semi-quantitative elemental analysis data of pyrrhotite grains and precipitates on their surface are presented in Figs. 14 and 15 and Table 15. Three types of physical features in varying amounts were identified on the surface of the analyzed grains: 1) flocculated material (Fig. 14a), 2) clusters of small needle-like, platelet and aggregate physical precipitates (Fig. 14b,c), and 3) thin, discontinuous gangue layers (Fig. 15). The flocculated material and surface gangue coatings are primarily silicates, whereas the physical precipitates are predominantly composed of Ca, O, Na, Si, K, and Cl (Table 15). The gangue layers were observed on pyrrhotite from all of the analyzed samples, however physical precipitates were only observed on a minor number of grains from the 0% RO and 40% RO samples.

7.2.4. Pentlandite

High-resolution SEM images and EDX elemental X-ray intensity maps of gangue layers on the surface of a pentlandite grain are presented in Fig. 16. Two types of physical features in varying amounts were identified on the surface of the analyzed pentlandite grains: 1) flocculated material, and 2) thin, discontinuous gangue layers (Fig. 16). The flocculated material and surface gangue coatings are primarily silicates, with a minor number of oxide coatings also identified on a few of the analyzed pentlandite grains. The gangue layers were observed on pentlandite from all of the analyzed samples.

8. Discussion

The process water (PW) had a lower concentration of dissolved species relative to thickener tank overflow water at the various degrees of reverse osmosis (RO) recirculation (0%, 20%, 40%, 60%, and 80%). The calcium, sulphate, copper, potassium, sodium, sulphite, TDS, total organic carbon (TOC), and total carbon (TC) concentrations and except for magnesium and total inorganic carbon (TIC), showed a linear concentration increase relative to the process water and thickener tank overflow water using reverse osmosis. In particular, the 40%, 60% and 80% RO samples showed high TDS concentrations (3388–4760 mg/L). This phenomenon is expected because when streams are recirculated, the concentration of species in solution and the TDS will increase. Higher concentrations of several species can cause inadvertent activation of non-sulphide and silicate gangue minerals, causing a decrease in selectivity (Liu et al., 2013). The higher TDS will decrease the bubble size resulting in a higher bubble surface area flux (Liu et al., 2013).

In contrast, the smaller bubbles increase the particle-bubble collision probability (Bourniva et al., 2012; Pugh et al., 1997), and particle-bubble attachment efficiencies (Hewitt et al., 1994). This phenomenon will change the flotation rate of both valuable and non-valuable minerals. High ionic strength solutions can also influence mineral flotation by surface passivation through the attachment of ions leading to depression and reducing collector-induced particle-bubble attachment probability (October et al., 2019).

There were no nickel and copper recoveries losses by recirculating thickener tank overflow water (0%, 20%, 40%, 60%, and 80% RO) relative to the process water. The nickel and copper recoveries (rougher-scavenger test) increased at a high percentage of RO recirculation (60% and 80%) relative to those obtained with process water. However, this occurred at the cost of lower nickel + copper grades. Chemical assays and examination of the flotation products identified pyrrhotite as one of the gangue minerals responsible for the lower grade. The cause for pyrrhotite recovery in all flotation tests identified by surface analysis

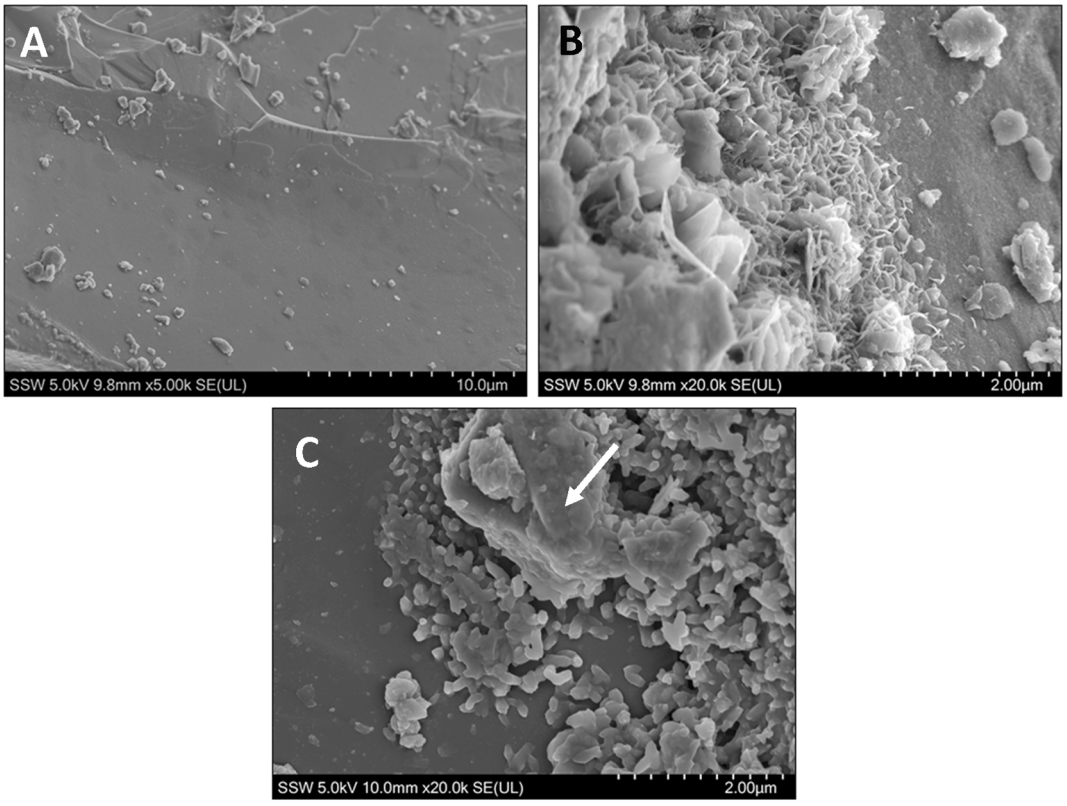

Fig. 14. High-resolution SEM images of surface particles and physical precipitates on pyrrhotite grains from the analyzed samples. (A) representative image of a clean grain surface with a minor amount of flocculated material (0% RO sample; 5000×). (B) Small needle-like and platelet crystals (0% RO sample; 20,000×). (C) Aggregate crystals that appear to have formed around flocculated material (white arrow) (40% RO sample; 20,000×) (combined primary rougher concentrates 1 and 2).

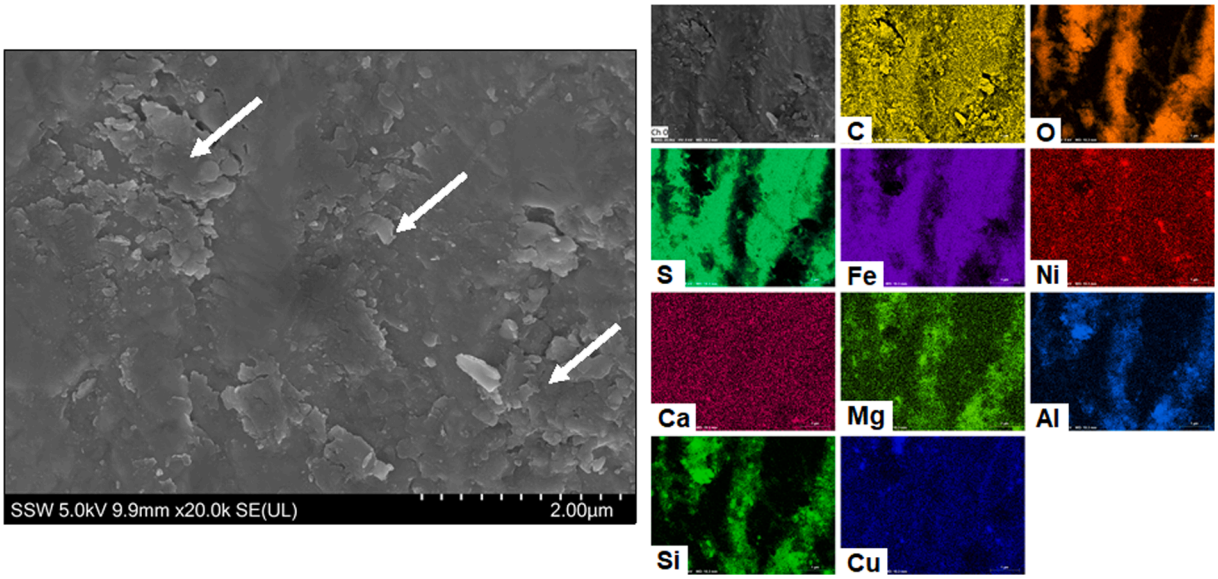

Fig. 15. BSE image and EDX element maps of thin gangue layers (white arrows) on a pyrrhotite grain from the 80% RO sample. The layer is predominantly composed of Si, O, Al, and Mg (combined primary rougher concentrates 1 and 2).

Table 15
EDX analyses of small needle-like crystals from the 0% RO sample (Fig. 12b), and aggregate crystals and clean pyrrhotite surface from the 40% RO sample (Fig. 12c). All data in wt.% (combined primary rougher concentrates 1 and 2).

Area of analysis	C	O	Na	Mg	Si	K	Ca	Cl	S	Fe	Ni
Small needle-like crystals	19.8	31.5	5.3	0.5	3.9	1.0	2.5	1.2	8.3	24.6	1.4
Aggregate crystals	14.7	25.5	4.7	0.7	1.6	2.3	10.4	–	23.8	16.4	–
Clean pyrrhotite surface	17.9	7.1	–	–	–	–	–	–	36.9	38.1	–

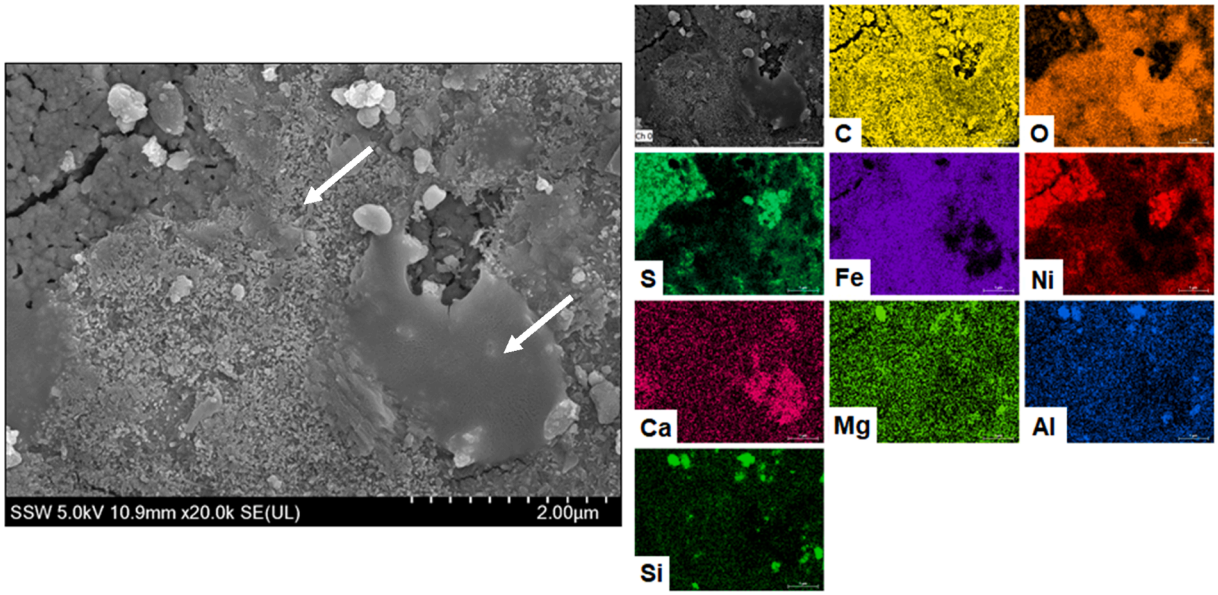

Fig. 16. BSE image and EDX element maps of thin gangue layers (white arrows) on a pentlandite grain from the 40% RO sample. The layers are predominantly composed of Fe, O, Mg, and Ca (combined primary rougher concentrates 1 and 2).

appeared to be linked to inadvertent activation by nickel, copper, and xanthate surface adsorption. However, the flotation tests showed that pyrrhotite recovery remained consistent regardless of the various degrees of thickener tank overflow water recirculation water (RO water) used in the test.

The ToF-SIMS and XPS surface analysis did not identify a clear link between an increase in ionic strength and a corresponding increase in the relative proportion of activating species on grain surfaces. Pyrrhotite surface analysis showed the presence of oxidative species (FeO_X, SO_X), gangue surface coatings, and physical precipitates identified in various proportions on grains from the samples investigated. Previous studies have shown that increasing concentrations of ions, such as calcium, can

negatively affect pyrrhotite flotation by adsorbing onto grain surfaces and creating a hydrophilic layer that inhibits xanthate adsorption (Multani and Waters, 2018). Ion products, such as calcium sulphate (e.g. gypsum), can also change the surface chemistry of minerals if they exceed the system's solubility level and precipitate in solution or nucleate on mineral surfaces. SEM/EDX analysis identified crystals composed of hydrophilic species, including calcium and oxygen, on the surface of pyrrhotite from the 0% and 40% RO samples. While the samples examined were from flotation concentrates, these passivating agents, when present in significant proportions, can inhibit pyrrhotite flotation by limiting activator and collector attachment and decreasing the hydrophobicity of pyrrhotite surfaces. Examination of grains from the tailings would likely reveal a higher relative proportion of these species on the pyrrhotite surfaces leading to their depression.

Interestingly, apart from elevated FeO and Ca species, surface analysis of pyrrhotite from the 80% RO concentrate suggested that the grains appeared to have relatively clean surfaces. The lack of surface species on the pyrrhotite surface may have led to higher recovery relative to process water. This lack of surface species on the pyrrhotite may be related to the high concentration of species in the 80% RO water which are partially fixed within the slurry and therefore no longer able to interact with the surface of the mineral phases.

The pyrrhotite flotation performance was probably due in part to the higher bubble surface area flux caused by the higher TDS. The higher TDS in the water will result in smaller bubble sizes and an increase in the overall number of bubbles, which will result in a higher bubble surface area flux (Liu et al., 2013; Levay and Schumann, 2006). This may have provided an opportunity for a more significant relative number of activated pyrrhotite grains to attach to bubbles and be recovered to the rougher concentrates (primary concentrate). Liu et al. (1993) determined that the number of bubbles increased from 100 for tap water to as high as 440 for recycled water and that the average bubble size for tap water was 2.9 mm compared to 1.9 mm for recycled water. These chemically induced physical changes to the bubble characteristics can significantly affect the flotation rate of both the value and non-value minerals. In this test work, the mineral recovery versus water recovery curve profiles for pyrrhotite and gangue were significantly different; similar to a typical flotation profile for pyrrhotite and linear for the gangue (non-sulphide gangue) minerals (Figs. 8 and 9). This data suggests that a greater portion of the recovered gangue (non-sulphide gangue) may have been through entrainment, whereas the pyrrhotite recovery may be more linked to inadvertent activation. As the TDS increased with the different %RO waters included in the flotation tests, there was no observed increase in the relative proportion of gangue (non-sulphide gangue) entrainment to the concentrates. This data indicates no linear link between the ionic strength of the solution and the degree of entrainment resulting from bubble size and surface area flux. It suggests that a reduction in bubble size reached its limit at the lower ionic strengths in the tests. Consistent bubble sizes and surface area fluxes allowed for a similar degree of froth drainage, resulting in consistent gangue removal across all tests.

The consistent recovery of pyrrhotite in the various tests performed may also be partially linked to the flotation pulp's ionic strength. One possible explanation is that an increase in solution ionic strength resulted in a change in the zeta-potential of pyrrhotite decreasing the adsorption capacity of activating species and collectors (October et al., 2019). If the change in zeta potential occurred at relatively low ionic strengths, the relative proportion of adsorbed species linked to flotation would be limited, beginning at the low %RO recirculation. This would constrain pyrrhotite's adsorption capacity in all the various %RO tests limiting the relative surface proportion of activators and collectors producing very similar flotation responses.

The gangue (non-sulphide gangue) was recovered due to entrainment and accidental activation by copper ions and xanthate species. The recovery of gangue (non-sulphide gangue) did not change between all the water types. This observation can be explained by the fact that copper and xanthate levels on the surface of analyzed gangue (non-sulphide gangue) grains were not significantly different between the six samples.

Regarding flotation kinetics, the ToF-SIMS, XPS and SEM/EDX data indicate, similar to the pyrrhotite, that pentlandite grains from the process water and 80% RO samples have cleaner surfaces relative to pentlandite from the 0%, 20%, 40% and 60% RO samples. As previously mentioned, calcium, sulph-oxy species and surface gangue layers increase the hydrophilicity of sulphide minerals, which may account for the reduced flotation kinetics of pentlandite observed for the 0%, 20%, 40% and 60% RO samples relative to the process water and 80% RO samples. Overall, pentlandite grains from the 0%, 20%, 40% and 60% RO samples showed a higher relative proportion of surface gangue material coverage compared to the process water and 80% RO samples, therefore it follows that those samples would show poorer flotation kinetics. The cleaner surfaces at 80% RO may be linked to the higher zeta-potential due to the higher concentration of solute (October et al., 2019). This will make the adsorption of ionic species and precipitates by pentlandite more difficult. Cleaner pentlandite surfaces and a greater relative proportion of elemental sulphur and polysulphides on pentlandite in the process water and 80% RO samples contributed at least in part to the faster flotation kinetics compared to those obtained with 0%, 20%, 40% and 60% observed during testing.

Another implication of thickener tank overflow water recirculation for the concentrator is that the increasing calcium species (656 mg/L for process water to 1754 for 80% RO) in a solution can increase pipe and equipment scaling, particularly at higher thickener tank overflow water recirculation. This is an existing issue for this particular concentrator, and increasing the thickener tank overflow water would potentially cause more frequent plant shutdowns resulting in significant financial impacts.

A point worth noting is that due to the lower pentlandite flotation kinetics obtained with 0%, 20%, 40%, 60% and 80% RO the pentlandite recovery will increase in the upper part of the rougher-scavenger circuit (lower recovery in the primary roughers and secondary roughers and higher recovery in the pyrrhotite roughers). This means that more pentlandite will report to the pyrrhotite rejection circuit (full flowsheet not shown in this article), which will incur pentlandite losses in the pyrrhtite rejection circuit since no circuit has a 100% recovery of paymetals. For this reason, water treatment will play a key role to clean the thickener tank overflow water and restore the flotation kinetics closer to that obtained with process water.

Water treatment of the thickener tank overflow prior to recirculation to the grinding circuit is required. The testing of various technologies (reverse osmosis, vacuum membrane distillation, etc.) and the percentage of the thickener tank overflow water treated will be part of a separate investigation. After completing the water treatment technologies testing in the laboratory, water treatment pilot plant testing will be done at the concentrator.

9. Conclusions

- Pyrrhotite flotation in the water types tested (process water, 0%, 20%, 40%, 60%, and 80% RO), was due in part to inadvertent activation by nickel, copper, and xanthate species.
- Pyrrhotite recovery for the RO water types was higher than that obtained for the process water.
  - This phenomenon was not caused by higher quantities of inadvertent species or collector on the pyrrhotite surfaces. The amount of these species on the pyrrhotite surfaces was similar between the samples.
  - The higher pyrrhotite recovery was most likely caused by smaller bubble size and higher bubble surface area flux generated by the higher TDS.
- Pyrrhotite recovery was similar at 0%, 20%, 40%, 60%, and 80% RO.

  - Adsorption of xanthate collector on pyrrhotite surfaces appears to be inhibited by the formation or concentration of surface oxidative species, fine gangue layers, calcium species, and physical precipitates. This may explain why the higher %RO samples (60% and 80% RO) did not result in higher pyrrhotite recovery relative to the lower %RO samples (0%, 20%, and 40% RO).
  - Pyrrhotite in the 80% RO sample appeared to have cleaner surfaces than pyrrhotite from the 0% and 40% RO and process water samples. Species may be fixed within the slurry and unavailable to interact with grain surfaces. Perhaps higher zeta-potential at higher solute concentrations may have resulted in lower ionic species and precipitate adsorption.
- The recovery of gangue (non-sulphide gangue) minerals for all the water types was caused by copper and xanthate species (inadvertent activation) and water recovery.
  - The recovery of gangue (non-sulphide gangue) remained constant for all the water types.
- The calcium, sulphate, calcium, copper, potassium, sodium, sulphite, TDS, total organic carbon (TOC), and total carbon (TC) concentrations were the lowest for the process water stream. These concentrations increased when the thickener tank overflow water was recirculated in reverse osmosis (RO).
- The following conclusions level can be made at the 95% confidence:
  - For the primary rougher concentrate 1
    - The nickel recoveries decreased (statistically significant) for 20% and 40% RO compared to that of process water.
    - The nickel recoveries for 0%, 60% and 80% RO was not significantly (statistical) affected compared to that obtained with process water.
    - The copper and non-sulphide gangue recoveries for 0%, 20%, 40%, 60%, and 80% RO were not significantly (statistical) affected compared to that obtained with process water.
  - For the primary rougher concentrate 2 (Kruskal-Wallis test was used)
    - The nickel and pyrrhotite recoveries were significantly (statistical) different between the water types tested (process water, 0%, 20%, 40%, 60%, and 80% RO).
    - The copper and gangue (non-sulphide gangue) recoveries were not significantly different between the water types tested (process water, 0%, 20%, 40%, 60%, and 80% RO).
  - The nickel and copper recoveries (rougher-scavenger test) for 60%, and 80% RO increased (statistically significant) compared to that of process water.
  - Flotation kinetics
    - The pentlandite flotation rate constants for 0%, 20%, 40%, 60%, and 80% RO were significantly (statistical) different from that obtained with process water.
    - The pyrrhotite flotation rate constants for 0%, 20%, 40%, and 80% RO were significantly (statistical) different from that obtained with process water. The P(z) value for 60% RO was 0.082; this value was slightly higher than 0.05.
    - The gangue flotation rate constants for 0%, 20%, 40%, 60% and 80% RO were not significantly (statistical) different from that obtained with process water.
- Cleaner pentlandite surfaces and the development of hydrophobic metal deficient sulphides, polysulphides, and elemental S species promoted faster flotation kinetics in the process water and 80% RO samples compared to the other four samples.
  - Pentlandite flotation may be hindered by the presence of hydrophilic species, including oxidative species and surface gangue layers, both of which appear to have contributed to the lower flotation kinetics observed for the 0%, 20%, 40%, and 60% RO samples.

Declaration of Competing Interest

The authors declare the following financial interests/personal relationships which may be considered as potential competing interests: Antonio Di Feo reports equipment, or supplies was provided by Glencore, Strathcona Mill. Antonio Di Feo reports a relationship with Glencore, Strathcona Mill that includes: non-financial support.

Acknowledgements

C.M. Hill-Svehla would like to thank Mark Biesinger and Ivan Barker for their assistance in conducting the XPS and FE-SEM/EDX analyses. Also, the authors would like to thank CanmetMINING for funding this project.

Appendix A

Maximum recovery for pentlandite (Pn) (R_m in %)

Process water versus 0% RO

$$\mu_{\text{difference}} = \text{abs}(-0.69) \tag{2}$$

$$\mu_{\text{difference}} > \text{abs}(-0.69) \tag{3}$$

Process water versus 20% RO

$$\mu_{\text{difference}} = \text{abs}(-2.20) \tag{4}$$

$$\mu_{\text{difference}} > \text{abs}(-2.20) \tag{5}$$

Process water versus 40% RO

$$\mu_{\text{difference}} = \text{abs}(-2.26) \tag{6}$$

$$\mu_{\text{difference}} > \text{abs}(-2.69) \tag{7}$$

Process water versus 60% RO

$$\mu_{\text{difference}} = \text{abs}(-3.28) \tag{8}$$

$$\mu_{\text{difference}} > \text{abs}(-3.28) \tag{9}$$

Process water versus 80% RO

$$\mu_{\text{difference}} = \text{abs}(-1.93) \tag{10}$$

$$\mu_{\text{difference}} > \text{abs}(-1.93) \tag{11}$$

Maximum recovery for pyrrhotite (Po) (R_m in %)

Process water versus 0% RO

$$\mu_{\text{difference}} = 0.04 \tag{12}$$

$$\mu_{\text{difference}} > 0.04 \tag{13}$$

Process water versus 20% RO

$$\mu_{\text{difference}} = 0.02 \tag{14}$$

$$\mu_{\text{difference}} > 0.02 \tag{15}$$

Process water versus 40% RO

$$\mu_{\text{difference}} = \text{abs}(-0.01) \tag{16}$$

$$\mu_{\text{difference}} > \text{abs}(-0.01) \tag{17}$$

Process water versus 60% RO

$$\mu_{\text{difference}} = \text{abs}(-0.35) \tag{18}$$

$$\mu_{\text{difference}} > \text{abs}(-0.035) \tag{19}$$

Process water versus 80% RO

$$\mu_{\text{difference}} = 0.12 \tag{20}$$

$$\mu_{\text{difference}} > 0.12 \tag{21}$$

Maximum recovery for non-sulphide gangue (Ga) (R_m in %)

Process water versus 0% RO

$$\mu_{\text{difference}} = 0.84 \tag{22}$$

$$\mu_{\text{difference}} > 0.84 \tag{23}$$

Process water versus 20% RO

$$\mu_{\text{difference}} = 0.83 \tag{24}$$

$$\mu_{\text{difference}} > 0.83 \tag{25}$$

Process water versus 40% RO

$$\mu_{\text{difference}} = \text{abs}(-0.15) \tag{26}$$

$$\mu_{\text{difference}} > \text{abs}(-0.15) \tag{27}$$

Process water versus 60% RO

$$\mu_{\text{difference}} = \text{abs}(-2.85) \tag{28}$$

$$\mu_{\text{difference}} > \text{abs}(-2.85) \tag{29}$$

Process water versus 80% RO

$$\mu_{\text{difference}} = \text{abs}(-0.11) \tag{30}$$

$$\mu_{\text{difference}} > \text{abs}(-0.11) \tag{31}$$

Flotation rate constant for pentlandite (Pn) (k in min^{-1})

Process water versus 0% RO

$$\mu_{\text{difference}} = 0.15 \tag{32}$$

$$\mu_{\text{difference}} > 0.15 \tag{33}$$

Process water versus 20% RO

$$\mu_{\text{difference}} = 0.22 \tag{34}$$

$$\mu_{\text{difference}} > 0.22 \tag{35}$$

Process water versus 40% RO

$$\mu_{\text{difference}} = 0.19 \tag{36}$$

$$\mu_{\text{difference}} > 0.19 \tag{37}$$

Process water versus 60% RO

$$\mu_{\text{difference}} = 0.19 \tag{38}$$

$$\mu_{\text{difference}} > 0.19 \tag{39}$$

Process water versus 80% RO

$$\mu_{\text{difference}} = 0.08 \tag{40}$$

$$\mu_{\text{difference}} > 0.08 \tag{41}$$

Flotation rate constant for pyrrhotite (Po) (k in min^{-1})

Process water versus 0% RO

$$\mu_{\text{difference}} = \text{abs}(-0.07) \tag{42}$$

$$\mu_{\text{difference}} > \text{abs}(-0.07) \tag{43}$$

Process water versus 20% RO

$$\mu_{\text{difference}} = \text{abs}(-0.05) \tag{44}$$

$$\mu_{\text{difference}} > \text{abs}(-0.05) \tag{45}$$

Process water versus 40% RO

$$\mu_{\text{difference}} = \text{abs}(-0.05) \tag{46}$$

$$\mu_{\text{difference}} > \text{abs}(-0.05) \tag{47}$$

Process water versus 60% RO

$$\mu_{\text{difference}} = \text{abs}(-0.04) \tag{48}$$

$$\mu_{\text{difference}} > \text{abs}(-0.04) \tag{49}$$

Process water versus 80% RO

$$\mu_{\text{difference}} = \text{abs}(-0.12) \tag{50}$$

$$\mu_{\text{difference}} > \text{abs}(-0.12) \tag{51}$$

Flotation rate constant for non-sulphide gangue (Ga) (k in min^{-1})

Process water versus 0% RO

$$\mu_{\text{difference}} = \text{abs}(-0.02) \tag{52}$$

$$\mu_{\text{difference}} > \text{abs}(-0.02) \tag{53}$$

Process water versus 20% RO

$$\mu_{\text{difference}} = 0.00 \tag{54}$$

$$\mu_{\text{difference}} > 0.00 \tag{55}$$

Process water versus 40% RO

$$\mu_{\text{difference}} = \text{abs}(-0.01) \tag{56}$$

$$\mu_{\text{difference}} > \text{abs}(-0.01) \tag{57}$$

Process water versus 60% RO

$$\mu_{\text{difference}} = 0.00 \tag{58}$$

$$\mu_{\text{difference}} > 0.00 \tag{59}$$

Process water versus 80% RO

$$\mu_{\text{difference}} = \text{abs}(-0.01) \tag{60}$$

$$\mu_{\text{difference}} > \text{abs}(-0.01) \tag{61}$$

$\mu_{difference}$

MANOVA

For the notation in this section, PW stands for process water. Also, μ stands for the mean of the variable in question. For example, $\mu_{\text{Ni rec}}$ signifies the mean of the nickel recovery.

Water Type (primary rougher concentrate 1):

Null hypothesis

$$\begin{pmatrix}\mu_{Ni}\\ \mu_{Cu}\\ \mu_{Po}\\ \mu_{Ga}\end{pmatrix} PW = \begin{pmatrix}\mu_{Ni}\\ \mu_{Cu}\\ \mu_{Po}\\ \mu_{Ga}\end{pmatrix} 0\%RO = \begin{pmatrix}\mu_{Ni}\\ \mu_{Cu}\\ \mu_{Po}\\ \mu_{Ga}\end{pmatrix} 20\%RO = \begin{pmatrix}\mu_{Ni}\\ \mu_{Cu}\\ \mu_{Po}\\ \mu_{Ga}\end{pmatrix} 40\%RO = \begin{pmatrix}\mu_{Ni}\\ \mu_{Cu}\\ \mu_{Po}\\ \mu_{Ga}\end{pmatrix} 60\%RO = \begin{pmatrix}\mu_{Ni}\\ \mu_{Cu}\\ \mu_{Po}\\ \mu_{Ga}\end{pmatrix} 80\%RO \tag{62}$$

Alternate hypothesis

The alternate hypothesis is that at least one recovery for a water type is significantly (95%) different to another recovery for another water type. For example, the mean nickel recovery for the process water (PW) is not equal to the mean nickel recovery for the 0% RO etc.

Orthogonal Contrast tests (primary rougher concentrate 1)

Differences among treatments can be done using orthogonal contrasts. Contrasts involve linear combinations of the variables (Johnson, 2019).

process water versus 0%RO

Null hypothesis

$$\begin{pmatrix}\mu_{Ni}\\ \mu_{Cu}\\ \mu_{Po}\\ \mu_{Ga}\end{pmatrix} PW = \begin{pmatrix}\mu_{Ni}\\ \mu_{Cu}\\ \mu_{Po}\\ \mu_{Ga}\end{pmatrix} 0\%RO \tag{63}$$

Alternate hypothesis

$$\begin{pmatrix}\mu_{Ni}\\ \mu_{Cu}\\ \mu_{Po}\\ \mu_{Ga}\end{pmatrix} PW \neq \begin{pmatrix}\mu_{Ni}\\ \mu_{Cu}\\ \mu_{Po}\\ \mu_{Ga}\end{pmatrix} 0\%RO \tag{64}$$

process water versus 20%RO

Null hypothesis

$$\begin{pmatrix}\mu_{Ni}\\ \mu_{Cu}\\ \mu_{Po}\\ \mu_{Ga}\end{pmatrix} PW = \begin{pmatrix}\mu_{Ni}\\ \mu_{Cu}\\ \mu_{Po}\\ \mu_{Ga}\end{pmatrix} 20\%RO \tag{65}$$

Alternate hypothesis

$$\begin{pmatrix}\mu_{Ni}\\ \mu_{Cu}\\ \mu_{Po}\\ \mu_{Ga}\end{pmatrix} PW \neq \begin{pmatrix}\mu_{Ni}\\ \mu_{Cu}\\ \mu_{Po}\\ \mu_{Ga}\end{pmatrix} 20\%RO \tag{66}$$

process water versus 40%RO

Null hypothesis

$$\begin{pmatrix} \mu_{Ni} \\ \mu_{Cu} \\ \mu_{Po} \\ \mu_{Ga} \end{pmatrix} PW = \begin{pmatrix} \mu_{Ni} \\ \mu_{Cu} \\ \mu_{Po} \\ \mu_{Ga} \end{pmatrix} 40\%RO \tag{67}$$

Alternate hypothesis

$$\begin{pmatrix} \mu_{Ni} \\ \mu_{Cu} \\ \mu_{Po} \\ \mu_{Ga} \end{pmatrix} PW \neq \begin{pmatrix} \mu_{Ni} \\ \mu_{Cu} \\ \mu_{Po} \\ \mu_{Ga} \end{pmatrix} 40\%RO \tag{68}$$

process water versus 60%RO

Null hypothesis

$$\begin{pmatrix} \mu_{Ni} \\ \mu_{Cu} \\ \mu_{Po} \\ \mu_{Ga} \end{pmatrix} PW = \begin{pmatrix} \mu_{Ni} \\ \mu_{Cu} \\ \mu_{Po} \\ \mu_{Ga} \end{pmatrix} 60\%RO \tag{69}$$

Alternate hypothesis

$$\begin{pmatrix} \mu_{Ni} \\ \mu_{Cu} \\ \mu_{Po} \\ \mu_{Ga} \end{pmatrix} PW \neq \begin{pmatrix} \mu_{Ni} \\ \mu_{Cu} \\ \mu_{Po} \\ \mu_{Ga} \end{pmatrix} 60\%RO \tag{70}$$

process water versus 80%RO

Null hypothesis

$$\begin{pmatrix} \mu_{Ni} \\ \mu_{Cu} \\ \mu_{Po} \\ \mu_{Ga} \end{pmatrix} PW = \begin{pmatrix} \mu_{Ni} \\ \mu_{Cu} \\ \mu_{Po} \\ \mu_{Ga} \end{pmatrix} 80\%RO \tag{71}$$

Alternate hypothesis

$$\begin{pmatrix} \mu_{Ni} \\ \mu_{Cu} \\ \mu_{Po} \\ \mu_{Ga} \end{pmatrix} PW \neq \begin{pmatrix} \mu_{Ni} \\ \mu_{Cu} \\ \mu_{Po} \\ \mu_{Ga} \end{pmatrix} 80\%RO \tag{72}$$

ANOVA

Nickel recovery

process water versus 0%RO

Null hypothesis

$$(\mu_{NiRec})PW = (\mu_{NiRec})0\%RO \tag{73}$$

Alternate hypothesis

$$(\mu_{NiRec})PW \neq (\mu_{NiRec})0\%RO \tag{74}$$

process water versus 20%RO

Null hypothesis

$$(\mu_{NiRec})PW = (\mu_{NiRec})20\%RO \tag{75}$$

Alternate hypothesis

$$(\mu_{NiRec})PW \neq (\mu_{NiRec})20\%RO \tag{76}$$

process water versus 40%RO

Null hypothesis

$$(\mu_{NiRec})PW = (\mu_{NiRec})40\%RO \tag{77}$$

Alternate hypothesis

$$(\mu_{NiRec})PW \neq (\mu_{NiRec})40\%RO \tag{78}$$

process water versus 60%RO

Null hypothesis

$$(\mu_{NiRec})PW = (\mu_{NiRec})60\%RO \quad (79)$$

Alternate hypothesis

$$(\mu_{NiRec})PW \neq (\mu_{NiRec})60\%RO \quad (80)$$

process water versus 80%RO

Null hypothesis

$$(\mu_{NiRec})PW = (\mu_{NiRec})80\%RO \quad (81)$$

Alternate hypothesis

$$(\mu_{NiRec})PW \neq (\mu_{NiRec})80\%RO \quad (82)$$

Copper recovery

process water versus 0%RO

Null hypothesis

$$(\mu_{CuRec})PW = (\mu_{CuRec})0\%RO \quad (83)$$

Alternate hypothesis

$$(\mu_{CuRec})PW \neq (\mu_{CuRec})0\%RO \quad (84)$$

process water versus 20%RO

Null hypothesis

$$(\mu_{CuRec})PW = (\mu_{CuRec})20\%RO \quad (85)$$

Alternate hypothesis

$$(\mu_{CuRec})PW \neq (\mu_{CuRec})20\%RO \quad (86)$$

process water versus 40%RO

Null hypothesis

$$(\mu_{CuRec})PW = (\mu_{CuRec})40\%RO \quad (87)$$

Alternate hypothesis

$$(\mu_{CuRec})PW \neq (\mu_{CuRec})40\%RO \quad (88)$$

process water versus 60%RO

Null hypothesis

$$(\mu_{CuRec})PW = (\mu_{CuRec})60\%RO \quad (89)$$

Alternate hypothesis

$$(\mu_{CuRec})PW \neq (\mu_{CuRec})60\%RO \quad (90)$$

process water versus 80%RO

Null hypothesis

$$(\mu_{CuRec})PW = (\mu_{CuRec})80\%RO \quad (91)$$

Alternate hypothesis

$$(\mu_{CuRec})PW \neq (\mu_{CuRec})80\%RO \quad (92)$$

Pyrrhotite recovery

process water versus 0%RO

Null hypothesis

$$(\mu_{PoRec})PW = (\mu_{PoRec})0\%RO \quad (93)$$

Alternate hypothesis

$$(\mu_{PoRec})PW \neq (\mu_{PoRec})0\%RO \quad (94)$$

process water versus 20%RO

Null hypothesis

$$(\mu_{PoRec})PW = (\mu_{PoRec})20\%RO \quad (95)$$

Alternate hypothesis

$$(\mu_{PoRec})PW \neq (\mu_{PoRec})20\%RO \quad (96)$$

process water versus 40%RO

Null hypothesis

$$(\mu_{PoRec})PW = (\mu_{PoRec})40\%RO \quad (97)$$

Alternate hypothesis

$$(\mu_{PoRec})PW \neq (\mu_{PoRec})40\%RO \quad (98)$$

process water versus 60%RO

Null hypothesis

$$(\mu_{PoRec})PW = (\mu_{PoRec})60\%RO \quad (99)$$

Alternate hypothesis

$$(\mu_{PoRec})PW \neq (\mu_{PoRec})60\%RO \quad (100)$$

process water versus 80%RO

Null hypothesis

$$(\mu_{PoRec})PW = (\mu_{PoRec})80\%RO \quad (101)$$

Alternate hypothesis

$$(\mu_{PoRec})PW \neq (\mu_{PoRec})80\%RO \quad (102)$$

Gangue recovery

process water versus 0%RO

Null hypothesis

$$(\mu_{GaRec})PW = (\mu_{GaRec})0\%RO \quad (103)$$

Alternate hypothesis

$$(\mu_{GaRec})PW \neq (\mu_{GaRec})0\%RO \quad (104)$$

process water versus 20%RO

Null hypothesis

$$(\mu_{GaRec})PW = (\mu_{GaRec})20\%RO \quad (105)$$

Alternate hypothesis

$$(\mu_{GaRec})PW \neq (\mu_{GaRec})20\%RO \quad (106)$$

process water versus 40%RO

Null hypothesis

$$(\mu_{GaRec})PW = (\mu_{GaRec})40\%RO \quad (107)$$

Alternate hypothesis

$$(\mu_{GaRec})PW \neq (\mu_{GaRec})40\%RO \quad (108)$$

process water versus 60%RO

Null hypothesis

$$(\mu_{GaRec})PW = (\mu_{GaRec})60\%RO \quad (109)$$

Alternate hypothesis

$$(\mu_{GaRec})PW \neq (\mu_{GaRec})60\%RO \quad (110)$$

process water versus 80%RO

Null hypothesis

$$(\mu_{GaRec})PW = (\mu_{GaRec})80\%RO \quad (111)$$

Alternate hypothesis

$$(\mu_{GaRec})PW \neq (\mu_{GaRec})80\%RO \tag{112}$$

Water Type (rougher-scavenger flotation):

Null hypothesis

$$\left(\frac{\mu_{NiRec}}{\mu_{CuRec}}\right)PW = \left(\frac{\mu_{NiRec}}{\mu_{CuRec}}\right)0\%RO = \left(\frac{\mu_{NiRec}}{\mu_{CuRec}}\right)20\%RO = \left(\frac{\mu_{NiRec}}{\mu_{CuRec}}\right)40\%RO = \left(\frac{\mu_{NiRec}}{\mu_{CuRec}}\right)60\%RO = \left(\frac{\mu_{NiRec}}{\mu_{CuRec}}\right)80\%RO \tag{113}$$

Alternate hypothesis

The alternate hypothesis is that at least one recovery for a water type is significantly (95%) different to another recovery for another water type. For example, the mean nickel recovery for the process water (PW) is not equal to the mean nickel recovery for the 0% RO etc.

Orthogonal Contrast tests (rougher-scavenger flotation)

Differences among treatments can be done using orthogonal contrasts. Contrasts involve linear combinations of the variables He, 2013(Johnson and Wicher, 2019).

process water versus 0%RO

Null hypothesis

$$\left(\frac{\mu_{NiRec}}{\mu_{CuRec}}\right)PW = \left(\frac{\mu_{NiRec}}{\mu_{CuRec}}\right)0\%RO \tag{114}$$

Alternate hypothesis

$$\left(\frac{\mu_{NiRec}}{\mu_{CuRec}}\right)PW \neq \left(\frac{\mu_{NiRec}}{\mu_{CuRec}}\right)0\%RO \tag{115}$$

process water versus 20%RO

Null hypothesis

$$\left(\frac{\mu_{NiRec}}{\mu_{CuRec}}\right)PW = \left(\frac{\mu_{NiRec}}{\mu_{CuRec}}\right)20\%RO \tag{116}$$

Alternate hypothesis

$$\left(\frac{\mu_{NiRec}}{\mu_{CuRec}}\right)PW \neq \left(\frac{\mu_{NiRec}}{\mu_{CuRec}}\right)20\%RO \tag{117}$$

process water versus 40%RO

Null hypothesis

$$\left(\frac{\mu_{NiRec}}{\mu_{CuRec}}\right)PW = \left(\frac{\mu_{NiRec}}{\mu_{CuRec}}\right)40\%RO \tag{118}$$

Alternate hypothesis

$$\left(\frac{\mu_{NiRec}}{\mu_{CuRec}}\right)PW \neq \left(\frac{\mu_{NiRec}}{\mu_{CuRec}}\right)40\%RO \tag{119}$$

process water versus 60%RO

Null hypothesis

$$\left(\frac{\mu_{NiRec}}{\mu_{CuRec}}\right)PW = \left(\frac{\mu_{NiRec}}{\mu_{CuRec}}\right)60\%RO \tag{120}$$

Alternate hypothesis

$$\left(\frac{\mu_{NiRec}}{\mu_{CuRec}}\right)PW \neq \left(\frac{\mu_{NiRec}}{\mu_{CuRec}}\right)60\%RO \tag{121}$$

process water versus 80%RO

Null hypothesis

$$\left(\frac{\mu_{NiRec}}{\mu_{CuRec}}\right)PW = \left(\frac{\mu_{NiRec}}{\mu_{CuRec}}\right)80\%RO \tag{122}$$

Alternate hypothesis

$$\left(\frac{\mu_{NiRec}}{\mu_{CuRec}}\right)PW \neq \left(\frac{\mu_{NiRec}}{\mu_{CuRec}}\right)80\%RO \tag{123}$$

ANOVA

Nickel recovery

process water versus 0%RO
Null hypothesis

$$(\mu_{NiRec})PW = (\mu_{NiRec})0\%RO \quad (124)$$

Alternate hypothesis

$$(\mu_{NiRec})PW \neq (\mu_{NiRec})0\%RO \quad (125)$$

process water versus 20%RO
Null hypothesis

$$(\mu_{NiRec})PW = (\mu_{NiRec})20\%RO \quad (126)$$

Alternate hypothesis

$$(\mu_{NiRec})PW \neq (\mu_{NiRec})20\%RO \quad (127)$$

process water versus 40%RO
Null hypothesis

$$(\mu_{NiRec})PW = (\mu_{NiRec})40\%RO \quad (128)$$

Alternate hypothesis

$$(\mu_{NiRec})PW \neq (\mu_{NiRec})40\%RO \quad (129)$$

process water versus 60%RO
Null hypothesis

$$(\mu_{NiRec})PW = (\mu_{NiRec})60\%RO \quad (130)$$

Alternate hypothesis

$$(\mu_{NiRec})PW \neq (\mu_{NiRec})60\%RO \quad (131)$$

process water versus 80%RO
Null hypothesis

$$(\mu_{NiRec})PW = (\mu_{NiRec})80\%RO \quad (132)$$

Alternate hypothesis

$$(\mu_{NiRec})PW \neq (\mu_{NiRec})80\%RO \quad (133)$$

Copper recovery
process water versus 0%RO
Null hypothesis

$$(\mu_{CuRec})PW = (\mu_{CuRec})0\%RO \quad (134)$$

Alternate hypothesis

$$(\mu_{CuRec})PW \neq (\mu_{CuRec})0\%RO \quad (135)$$

process water versus 20%RO
Null hypothesis

$$(\mu_{CuRec})PW = (\mu_{CuRec})20\%RO \quad (136)$$

Alternate hypothesis

$$(\mu_{CuRec})PW \neq (\mu_{CuRec})20\%RO \quad (137)$$

process water versus 40%RO
Null hypothesis

$$(\mu_{CuRec})PW = (\mu_{CuRec})40\%RO \quad (138)$$

Alternate hypothesis

$$(\mu_{CuRec})PW \neq (\mu_{CuRec})40\%RO \quad (139)$$

process water versus 60%RO

Null hypothesis

$$(\mu_{CuRec})PW = (\mu_{CuRec})60\%RO \tag{140}$$

Alternate hypothesis

$$(\mu_{CuRec})PW \neq (\mu_{CuRec})60\%RO \tag{141}$$

process water versus 80%RO

Null hypothesis

$$(\mu_{CuRec})PW = (\mu_{CuRec})80\%RO \tag{142}$$

Alternate hypothesis

$$(\mu_{CuRec})PW \neq (\mu_{CuRec})80\%RO \tag{143}$$

Kruskal-Wallis test

Null hypothesis

$$\begin{pmatrix}\mu_{Ni}\\ \mu_{Cu}\\ \mu_{Po}\\ \mu_{Ga}\end{pmatrix}PW = \begin{pmatrix}\mu_{Ni}\\ \mu_{Cu}\\ \mu_{Po}\\ \mu_{Ga}\end{pmatrix}0\%RO = \begin{pmatrix}\mu_{Ni}\\ \mu_{Cu}\\ \mu_{Po}\\ \mu_{Ga}\end{pmatrix}20\%RO = \begin{pmatrix}\mu_{Ni}\\ \mu_{Cu}\\ \mu_{Po}\\ \mu_{Ga}\end{pmatrix}40\%RO = \begin{pmatrix}\mu_{Ni}\\ \mu_{Cu}\\ \mu_{Po}\\ \mu_{Ga}\end{pmatrix}60\%RO = \begin{pmatrix}\mu_{Ni}\\ \mu_{Cu}\\ \mu_{Po}\\ \mu_{Ga}\end{pmatrix}80\%RO \tag{144}$$

Alternate hypothesis

The alternate hypothesis is that at least one recovery for a water type is significantly (95%) different to another recovery for another water type. For example, the mean nickel recovery for the process water (PW) is not equal to the mean nickel recovery for the 0% RO etc.

References

Becker, M., de Villiers, J., Bradshaw, D., 2010. The flotation of magnetic and non-magnetic pyrrhotite from selected nickel ore deposits. Miner. Eng. 23, 1045–1052.

Biçak, O., Ekmekçi, Z., Can, M., Öztürk, Y., 2012. The effect of water chemistry on froth stability and surface chemistry of the flotation of a Cu-Zn sulfide ore. Int. J. Miner. Process. 102–103, 32–37.

Bournival, G., Pugh, R.J., Ata, S., 2012. Examination of NaCl and MIBC as bubble coalescence inhibitor in relation to froth flotation. Miner. Eng. 25, 47–53.

Carlson, L., Bigham, J.M., Schwertmann, U., Kyek, A., Wagner, F., 2002. Scavenging of As from Acid Mine Drainage by Schwertmannite and Ferrihydrite: A Comparison with Synthetic Analogues. Environ. Sci. Technol. 36, 1712–1719.

Di Feo, A., Mortazavi, S., Langley, S., Morin, L., Prabhakar, G., Demers, A., Bedard, I., Volchek, K., 2020. The Effects of Water Recycling on Flotation at a North American Concentrator-Part 1. Journal of Minerals and Materials Characterization and Engineering 8, 240–276.

Ekmekçi, Z., Becker, M., Bagci Tekes, E., Bradshaw, D., 2010. The relationship between the electrochemical, mineralogical and flotation characteristics of pyrrhotite samples from different Ni ores. J. Electroanal. Chem. 647, 133–143.

He, F., 2013. Nonparametric MANOVA Approaches for non-normal Multivariate Outcomes, Doctor of Philosophy. University of Pittsburgh.

Hewitt, D., Fornasiero, D., Ralston, J., 1994. Bubble particle attachment efficiency. Miner. Eng. 7, 657–665.

Ikumapayi, F., Makitalo, M., Johansson, B., Rao, K.H., 2012. Recycling of process water in sulphide flotation: effect of calcium and sulphate ions on flotation of galena. Miner. Eng. 39, 77–88.

Johnson, R.A., Wichern, D.W., 2019. Applied Multivariate Statistical Analysis, 6th ed.

Kelebek, S., Nanthakumar, B., Katsabanis, P.D., 2007. Oxidation of Complex Ni-Cu Sulphide Ores and its implication for flotation practice. Can. Metall. Q. 46, 279–284.

Le, T.M.K., Mäkelä, M., Schreithofer, N., Dahl, O., 2020. A multivariate approach for evaluation and monitoring of water quality in mining and minerals processing industry. Miner. Eng. 157, 106582.

Levay, G., and Schumann, R., A Systematic Approach to Water Quality Management in the Minerals Processing Industry, Water in Mining Conference, Brisbane, QLD, November 14 to 16, 2006.

Levay, G., Smart, R.S.T.C., Skinner, V.M., 2001. The impact of water quality on flotation performance. The Journal of the South African Institute of Mining and Metallurgy, March/April.

Liu, W., Moran, C.J., Vink, S., 2013. A review of the effect of water quality on flotation. Miner. Eng. 53, 91–100.

Liu, L., Rao, S.R., Finch, J.A., 1993. Laboratory study of effect of recycle water on flotation of a Cu/Zn sulphide ore. J. S. Afr. Inst. Min. Metall. 6 (11), 1183–1190.

Malaeb, L., Ayoub, G.M., 2011. Reverse osmosis technology for water treatment: state of the art review. Desalination 267, 1–8.

Multani, R.S., Waters, K.E., 2018. A review of the physiochemical properties and flotation of pyrrhotite superstructures (4C – Fe_7S_8 / 5C – Fe_9S_{10}) in Ni-Cu sulphide mineral processing. Can. J. Chem. Eng. 96, 1185–1206.

Muzenda, E., 2010. An investigation into the effect of water quality on flotation performance. Int. J. Chem., Mol., Nucl. Mater. Metall. Eng. 4 (9).

Napier-Munn, T.J., 2012. Statistical methods to compare batch flotation grade-recovery curves and rate constants. Miner. Eng. 34, 70–77.

October, L., Corin, K., Schreithofer, N., Manono, M., Wiese, J., 2019. Water quality effects on bubble-particle attachment of pyrrhotite. Miner. Eng. 131, 230–236.

Pugh, R.J., Weissenborn, P., Paulson, O., 1997. Flotation in inorganic electrolytes; the relationship between recover of hydrophobic particles, surface tension, bubble coalescence and gas solubility. Int. J. Miner. Process. 51, 125–138.

Rao, R., Finch, J.A., 1989. A Review of Water re-use in Flotation. Miner. Eng. 2, 65–85.